Physics – Uspekhi **38** (10) 1099 – 1118 (1995)

PACS numbers: 62.60. + v; 42.25.Jh; 43.35.Bf; 43.80.Gx

Thermal self-action of acoustic wave packets in a liquid

F V Bunkin, G A Lyakhov, K F Shipilov

Contents

Abstract. A review is given of theoretical and experimental investigations of the propagation of powerful ultrasonic beams in high-viscosity liquids. Calculations are reported of the conditions for the observation of spatial and temporal self-compression of a wave packet as a result of sound-induced heating of a liquid. An account is given of theoretical predictions and of quantitative agreement of these predictions with experimental results on the effects of self-focusing of ultrasonic beams and of sound-induced transparency of viscous liquids. More than tenfold increase in the peak intensity of an ultrasonic pulse in the focal region, of dimensions of the order of three or four wavelengths, has been achieved under optimal conditions. Physical and biological applications of the observed effects of controlled self-action of ultrasonic waves in the bulk of a viscous liquid are discussed.

1. Introduction

A wave of finite amplitude A propagating through a medium changes various parameters of this medium and in particular its refractive index n (and, consequently, the intrinsic phase velocity v) in the region of its propagation. If $\partial n/\partial A < 0$, the rays forming a wave packet become defocused and the dimensions of the packet increase. The action of nonlinear defocusing supplements the diffraction and dispersion spreading typical of wave packets (and independent of the amplitude). However, if $\partial n/\partial A > 0$, the peripheral rays overcome diffraction and contract towards the centre of a packet, so that self-focusing takes place. This is an effect common to waves of any nature [1] and it has been investigated in detail very successfully in the optical range [2 – 5].

Obvious attractive applications can be based on the concentration, associated with such self-focusing, of the energy of a wave packet (naturally, it is understood that the total energy is conserved) in a narrow space – time region. Not only an increase in the effectiveness of many physical processes, due to an increase in the wave intensity in a small region, but also qualitatively new effects above a certain intensity threshold may, in principle, be observed in a self-focusing region. However, in the optical range, investigated in much greater detail than other ranges, these opportunities are limited. First, a strong increase in the intensity activates also effects that compete with self-focusing, for example, an electron avalanche and the resultant mechanical damage to a medium [6]. Second, it is difficult to control self-focusing because of the fairly stringent conditions for achieving it. The requirement for exceeding a certain threshold value of the laser beam power together with the short times needed for the establishment of a nonlinear susceptibility (which is true, for example, of the Kerr mechanism) make it necessary to use sources generating nanosecond and subpicosecond pulses. In the case of these pulses it is rather difficult to ensure a smooth intensity distribution in a transverse section of a beam, but such a distribution is essential to avoid accidental beam filamentation, observed in the very first experiment on self-focusing of light [7]. Third, applications

F V Bunkin, G A Lyakhov, K F Shipilov Institute of General Physics, Russian Academy of Sciences, ul. Vavilova 38, 117942 Moscow
Tel. (095) 135 82 34. E-mail: shipilov@wpd.gpi.msk.su

Received 14 December 1994; revision received 26 January 1995
Uspekhi Fizicheskikh Nauk **165** (10) 1145 – 1164 (1995)
Translated by A Tybulewicz

are greatly hindered by the independent problem of recording the effects, which requires development of special high-resolution high-speed photographic methods.

The first observation of self-focusing of acoustic waves [8] has been delayed by other factors [9].

Nonlinear acoustics has a much longer history than nonlinear optics. At the beginning of this century important physical and applied results were obtained by nonlinear acoustic methods [10]. It was established immediately that the dominant nonlinear mechanism in the acoustics of longitudinal waves is elastic and that the effects can be both odd and even in respect of the amplitude. In the case of liquid media, this gives rise to the first difference from transverse optical waves, because the isotropic symmetry forbids the quadratic and all even (in respect of the field) effects, so that self-focusing of light is observed, for example, because of the cubic nonlinearity. The second important distinction between nonlinear acoustics and nonlinear optics is the usually weak acoustic dispersion: the velocity of sound in common liquids is practically independent of its frequency in the kilohertz and megahertz ranges. A consequence of this is a high efficiency of nonlinear frequency conversion in acoustics: in view of the equality of the phase velocities, the incident wave transfers, over the whole propagation path, energy efficiently to the waves generated because of the nonlinearity. This process, universal in acoustics, of dispersion-unhindered enrichment with the harmonics leads to the formation of a shock wave at a finite distance L_d traversed by a wave in a liquid medium (in nonlinear acoustics this is known as the discontinuity-formation length) [10]. Moreover, a redistribution of the intensity from the periphery to the centre is also possible [11], but fast dissipation of the acoustic energy which accompanies the formation of a shock wave excludes potential applications requiring a regular increase in the intensity.

The formation of a shock wave is the result of a quadratic nonlinearity with a short formation time. Therefore, the quantity L_d is inversely proportional to the input amplitude and practically independent of the duration of the acoustic interaction with a liquid medium. This provides the first suggestions as to how to achieve self-focusing of sound, which can be described comprehensively by the spatial scale L_f of its growth, known as the self-focusing length. In view of the universal nature of the process of formation of a shock wave, there is an obvious condition that $L_d > L_f$. The only hope is in the inelastic mechanisms of nonlinearity. A close analogy with nonlinear optics [12] shows that self-focusing is due to a cubic nonlinearity, but it is also obvious that, within the framework of one mechanism, this nonlinearity is much weaker than the quadratic one and this is true up to the sound intensities causing damage to a medium. However, if a nonlinearity is of other (than inelastic) physical origin, it is possible to satisfy the inequality $L_d > L_f$ because of, first, a stronger ($L_f \propto A^{-2}$) dependence of the effectiveness of the cubic nonlinearity on the acoustic wave amplitude. A second reason is the possibility of cumulation of nonlinear changes in the velocity with time, which is typical of diffusion mechanisms, when L_f is inversely proportional to the energy of a wave, i.e. $L_f \propto (A^2\tau)^{-2}$, where τ is the duration of an acoustic pulse.

Recent theoretical and experimental investigations have shown above all that the sought-after effective nonlinear mechanism does exist: it is the change in the velocity of sound as a result of heating of the propagation medium by a wave. [9, 13] The effect of the concentration mechanism in familiar solutions is less and the competition of the generation of harmonics and other nonlinear mechanisms destroying a wave packet cannot be overcome [14]. Moreover, it is not clear whether one could use for this purpose the electroacoustic (in polarisable dielectric liquids) [15] and magnetoacoustic (in magnetic liquids) [16] mechanisms.

Practically immediately after the experiments reported in Ref. [13], and as a continuation of them, a new effect was observed. By analogy with the optical transparency it was called the acoustic self-induced transparency [17]. This effect represents a change, as a result of sound-induced heating, not only in the velocity of sound, but also in its absorption in the insonated liquid. Its main manifestation is an increase, with the increase in the input intensity, of the depth of penetration of sound into an absorbing liquid. It can be observed also in highly viscous liquids, but in a limited temperature range where the temperature derivative of the absorption coefficient is negative: $\partial\delta/\partial T < 0$. Outside this range, we have $\partial\delta/\partial T > 0$ and the depth of penetration of sound decreases with the increase in its input intensity; one could naturally speak here of the self-induced darkening [18]. The self-induced transparency has two effects: first, it increases the efficiency of self-focusing; second, its action has a significant influence also on the time envelope of a packet and under certain conditions it gives rise to a smooth short high-intensity pulse [18]. Its action thus facilitates directly the concentration of acoustic energy in a compressed wave packet.

Experiments [13, 17, 18] show that the self-focusing of sound is, in contrast to its optical analogue, a fairly easily controlled process. This is extremely important in applications, especially as this happens under theoretically predicted conditions. The control and monitoring can be performed (once again, this is different from the actual situation in nonlinear optics) by fully reliable and accurate methods involving the use of quasipoint-like acoustic probes and also of optical techniques [17, 19].

This effectiveness and ease of control of the thermal self-action of sound in a liquid makes it possible to suggest a whole range of applications of this effect. Naturally, special attention has been given to biological and medical applications, since the majority of biotissues have physical properties typical of weakly inhomogeneous highly viscous liquids.

Second 2 deals with the theory of self-focusing and self-induced transparency of sound in a liquid due to the thermal nonlinearity. The purpose of the theory is here to identify the conditions for observing these effects against the background of competing and suppressing effects, and to estimate the effectiveness of these effects in a real range of material parameters of liquid media for real acoustic sources. Section 3 describes practically all the experiments on the thermal self-action of sound carried out in well-known laboratories. Promising applications of the new effects, which are currently under development, are discussed in Section 4.

2. Theory of the thermal self-action of sound

Many liquids satisfy the condition of a monotonic reduction in the velocity of sound with increase in temperature, which is essential for the observation of the first of the self-action effects, which is the thermal self-focusing of sound. The exceptions are water (at temperatures below 74.5 °C) and a number of liquid materials: bismuth, antimony, and tellurium. However, it is more difficult to satisfy the thresholds relating to the parameters of a medium and of an acoustic beam. Estimates [20] for steady (i.e. for insonation times longer than all the times representing the establishment of the nonlinear parameters of a medium) self-focusing show that the threshold condition can indeed be satisfied. However, the temperature distribution in typical liquids is established in not less than 10^2 s under the action of acoustic beams of centimetre radius and this time is sufficient for the growth of beam-destroying sound-induced convection [21]. Therefore, in estimating the conditions sufficient for self-focusing, including the conditions for separating it from the background of the competing nonlinear processes, it is necessary to turn to the theory of transient effects.

2.1 Time-dependent equations for the self-action of sound

Nonlinear acoustic effects in homogeneous absorbing media can be described by a system of thermohydrodynamic equations, including the equation of continuity

$$\partial_t \rho + \partial_b(\rho v_b) = 0\,. \tag{1}$$

the equation of the balance of forces

$$\rho(\partial_t + v_b\,\partial_b)v_a + \partial_a p = \eta\,\partial_b^2 v_a + \left(\zeta + \frac{\eta}{3}\right)\partial_a\partial_b v_b\,, \tag{2}$$

and the equation of entropy production

$$\rho T(\partial_t + v_b\,\partial_b)S - \varkappa\,\partial_b^2 T = \zeta(\partial_b v_b)^2 + \eta\,\partial_a v_b\left(\partial_a v_b + \partial_b v_a - \tfrac{2\delta_{ab}}{3}\,\partial_c v_c\right), \tag{3}$$

Here ρ, p, T, S are, respectively, the mass density of the investigated liquid, the pressure, temperature, and the entropy density; v_a is a Cartesian component of the velocity; η, ζ, and $\varkappa$ are, respectively, the shear viscosity, the bulk viscosity, and the thermal conductivity; ∂_t, ∂_a, ∂_b, ∂_c are the partial derivatives with respect to the variables indicated by the subscripts; δ_{ab} is the Kronecker delta. The same letters (ρ, p, T, S) will be used later to denote deviations of these quantities from their equilibrium values identified by the subscript zero.

The system of equations (1)–(3) is closed by the equation of state, i.e. by the dependences $\rho(p, T)$ and $S(p, T)$. As pointed out in the Introduction, we shall assume that all the spatial scales of the growth of the investigated effects (in our case this is particularly the self-focusing length L_f) are shorter than the distance L_d in which a discontinuity forms [10]:

$$L < L_d = (\rho c_0^5)^{1/2}(2I_0)^{-1/2}(\omega\varepsilon)^{-1}\,, \tag{4}$$

Here, ω is the frequency of the acoustic beam, I_0 is its input intensity; $\varepsilon = 1 + (1/\rho_0)[(\partial c/\partial p)_T + \alpha T_0(\partial c/\partial T)_p/\rho_0 c_p]$ is the elastic nonlinear coefficient; α is the volume thermal expansion coefficient; c_0 is the equilibrium velocity of sound; c_p is the isobaric specific heat. If inequality (4) is not obeyed, it does not mean that the thermal self-focusing effect cannot occur, but the situation becomes more complex (particularly if the self-focusing takes place, a discontinuity should form faster on the beam axis than at the periphery) and, consequently, it becomes less informative.

If we assume that inequality (4) is satisfied, we can solve the problem in the quasimonochromatic approximation. The unperturbed solution is that of the linearised, close to the state of equilibrium, system of equations (1)–(3) together with the following linearised equations of state:

$$\rho = \left(\frac{1}{c_0^2} + \frac{\alpha T_0}{c_p}\right)p - \rho_0\alpha T\,, \qquad S = -\frac{\alpha}{\rho_0}\,p + \frac{c_p}{T_0}\,T\,. \tag{5}$$

The dispersion equation has two solutions; $\omega = 0$ and $\omega = c_0\boldsymbol{k}$ (the wave vector $\boldsymbol{k}$ is directed along the x axis). The complex amplitudes T^ω, p^ω, v_x^ω, $v_\perp^\omega = (0, v_t, v_z)$ are linked by the following relationships:

$$T^\omega = \frac{\alpha T_0}{\rho_0 c_p}\,p^\omega\,, \quad v_x = \frac{p^\omega}{\rho_0 c_0}\,, \quad v_\perp^\omega = -(\mathrm{i}\omega\rho_0)^{-1}\nabla_\perp p^\omega\,. \tag{6}$$

The solution of the nonlinear problem should now be sought in the form

$$p = p^0 + \frac{p^\omega}{2}\exp\left[\mathrm{i}\omega\left(t - \frac{x}{c_0}\right)\right] + \text{c.c.} \tag{7}$$

and similarly for the variables T and v_a on the assumption that p^0, p^ω, T^0, T^ω, v_a^0, v_a^ω (the superscript 0 corresponds to $\omega = 0$) are slowly varying functions:

$$\partial_t \propto \mu\,, \quad \partial_x \propto \mu\,, \quad \nabla_\perp = (0, \partial_y, \partial_z) \propto \mu^{1/2}, \quad \mu \ll 1\,.$$

This is the well-known parabolic approximation used in the nonlinear theory of diffraction [3]. Its applicability to our problem is determined by the values of a whole range of parameters. First of all, the inequality (4) must be obeyed. Next, the changes in the input amplitude of sound should be slow over a distance of one wavelength (beam width $a > 2\pi c_0/\omega$, pulse duration $\tau > \omega^{-1}$) and the deviations from equilibrium should be small: $T/T_0 \ll 1$, $v_a/c_0 \ll 1$, etc. The condition of weak dissipation is represented by the inequalities $(\tilde\zeta; \tilde\eta) = (\omega/\rho_0 c_0^2)(\zeta; \eta) \ll 1$ (the coefficient of absorption of sound over a distance of one wavelength is less than unity) and $\tilde\varkappa = \omega\varkappa/\rho_0 c_0 c_p \ll 1$ (the diffusion spreading time of a temperature perturbation in a region of size of one wavelength is much greater than the period of acoustic oscillations). The last two inequalities are readily satisfied in the ultrasonic range: at $T_0 = 20$ °C when the frequency is $\omega/2\pi = 2$ MHz, the corresponding values of $\tilde\varkappa$ are 3.5×10^{-7} for benzene ($\tilde\eta = 5 \times 10^{-6}$) and 1.6×10^{-7} for the more viscous glycerine ($\tilde\eta = 4 \times 10^{-3}$). (Here and later we shall use tabulated values given in Ref. [22].)

Substitution of relationships (6) and (7) into Eqns (1)–(3) and separation of the terms with frequencies $\omega = 0$ and $\omega = c_0\boldsymbol{k}$ gives a system of reduced equations that describe the self-action of sound.

The equation for the changes in the amplitude of the acoustic pressure is

$$\left(c_0\,\partial_x + \partial_t + \frac{\mathrm{i}c_0^2\nabla_\perp}{2\omega} + c_0\delta\right)p^\omega = \mathrm{i}\omega p^\omega\left[\frac{v_x}{c_0} + \frac{(1-a_1)|p^\omega|^2}{8(\rho_0 c_0^2)^2} - \frac{a_2 p^0}{\rho_0 c_0^2} - \frac{a_3 T^0}{T_0}\right]. \tag{8}$$

The absorption coefficient, derived taking account only of the classical viscous mechanism, is $\delta = (\zeta + 4\eta/3)\omega^2/\rho_0 c_0^3$. The remaining coefficients a_i are governed solely by the elastic nonlinear coefficient ε and by the derivative of the velocity of sound with respect to T: $a_1 \approx (\varepsilon - 1)^2/2$, $a_2 \approx \varepsilon - 1$, $a_3 \approx T_0\gamma_p/2$, where $\gamma_p = (\partial \ln c^2/\partial T)_p$.

The terms on the right of Eqn (8) correspond to four mechanisms of the self-action of sound: the excitation of longitudinal flow, somewhat delayed changes in the state under the action of the elastic mechanism, generation of video-frequency pressure pulses (acoustic detection), and heating of a liquid by sound.

The activation of flow is determined by the total attenuation of sound caused by dissipation and diffraction:

$$(\partial_t - \nu\nabla_\perp^2)v_x^0 + \rho_0^{-1}\partial_x p^0 = \frac{(c_0\partial_x + \partial_t)|p^\omega|^2}{4\rho_0^2 c_0^3}, \qquad (9)$$

where $\nu = \eta/\rho_0$.

Heating is also due to two mechanisms, which are viscous and adiabatic:

$$(\partial_t - \chi\nabla_\perp^2)T^0 - q\,\partial_t p^0 = \frac{\delta|p^\omega|^2}{\rho_0^2 c_0 c_p} - \frac{T_0 a_4\,\partial_t|p^\omega|^2}{(2\rho_0 c_0^2)^2}. \qquad (10)$$

Here, $\chi = \varkappa(\rho_0 c_0^2)^{-1}$ is the thermal diffusivity and $a_4 \approx \alpha c_0^2/c_p$. Finally, acoustic detection is the result of dissipative and adiabatic processes [9].

2.2 Comparative estimates of the effectiveness of the various nonlinear mechanisms

The possibility of observing the self-focusing can be determined by investigating the system of equations (8)–(10) using the results of calculations of the optical analogue of the self-focusing in the aberration-free approximation [3]. We shall report numerical estimates for benzene and glycerine at $T_0 = 20$ °C for $\omega/2\pi = 2$ MHz. At room temperature this value is far from the relaxation frequencies for either of the two selected liquids. The radius of an acoustic beam is assumed to be $a = 0.75$ cm.

In the instantaneous mechanism the focusing length is

$$L_f = \frac{a}{2}\left(\frac{c_0}{\Delta c}\right)^{1/2}, \qquad (11)$$

where $\Delta c = \varepsilon^2 I/(8\rho_0 c^2)$ is the nonlinear change in the velocity of sound. Comparison of expressions (4) and (11) shows that the ratio of the relevant lengths is $L_f/L_d = 4\pi a/\lambda > 1$ ($\lambda = 2\pi c_0/\omega$ is the wavelength of sound). Therefore, this mechanism cannot result in self-focusing. The reason is quite obvious; both processes (formation of a discontinuity and self-focusing of a beam) are due to the same nonlinearity, but the former is not associated with the bounded nature of the beam, whereas the second is of diffraction origin.

Other mechanisms are generally transient. The time for their establishment can readily be estimated from Eqns (8)–(10):

$$\tau_v = \frac{a^2}{\nu}, \quad \tau_p = \frac{a}{c_0}, \quad \tau_T = \frac{a^2}{\chi}.$$

Numerical values of these times form a definite sequence in the case of benzene and glycerine:

$$\tau_T = (4.5 \text{ to } 4.7)\times 10^2 \text{ s} \gg \tau_v = 6.1 \text{ to } 0.04 \text{ s} \gg \tau_p = (6.6 \text{ to } 4.5)\times 10^{-6} \text{ s}.$$

Therefore, throughout the whole real range of τ, the contribution to the self-action of an acoustic beam, important against the background of a growing shock wave, can only come from sound-induced flow and heating.

We shall now compare the effectiveness of the viscous (T_δ^0) and adiabatic (T_α^0) heating. Under steady-state conditions, it follows from Eqn (10) that

$$T_\delta^0 = \frac{2\delta I\tau}{\rho_0 c_p}, \quad T_\alpha^0 = \frac{\alpha T_0 I}{2\rho_0 c_p c_0}, \qquad (13)$$

which leads to $T_\delta^0/T_\alpha^0 \gg 1$, i.e. only the contribution of viscous heating is of practical importance if we consider media with the absorption coefficient $\delta > 10^{-2} - 10^{-3}$ cm^{-1} when the acoustic pulse duration exceeds $(1-10)\omega^{-1}$.

The excitation of flow is related to two factors. The maximum flow velocity, governed by the attenuation of sound under steady ($\tau > \tau_v$) and unsteady ($\tau < \tau_v$) conditions can be estimated on the basis of Eqns (9) and (10):

$$v_\delta^0 \approx \frac{a^2\delta I}{\eta c_0}, \quad v_d^0 \approx \frac{\delta I\tau}{\rho_0 c_p}. \qquad (14)$$

In the absence of dissipation, the diffraction attenuation should set a liquid in motion up to a velocity v_s^0 and the maximum value of this velocity is governed by the dependence $I(x) = I(0)/[1 + (x/L_s)^2]$, where L_s is the diffraction scale of the spreading of a beam, which in the absence of the self-action is equal to $\omega a^2/c_0$. It then follows from Eqn (9) that

$$v_d^0 \approx \frac{I\tau}{2\rho_0 c_0 L_s a}, \quad \tau < \tau_v,$$
$$v_d^0 \approx \frac{a^2 I}{2\eta c_0 L_s}, \quad \tau > \tau_v. \qquad (15)$$

The ratio v_δ^0/v_s^0 is in both cases equal to $2\delta/L_s$ and, in principle, it can assume values of the order of unity, i.e. the contributions of the dissipative and diffraction sources of flow can formally be comparable in magnitude. However, in finding the self-focusing threshold we have to assume that $L_s \to \infty$, since at the threshold the diffraction spreading is, by definition, compensated by the nonlinear refraction. Therefore, in estimating the possibility of self-focusing we should consider only a viscous source of sound-induced flow.

In liquids with a finite viscosity it is found that forced convection might not destroy, but it can distort considerably the process of steady self-focusing. The steady convection velocity can be estimated when the gravitational force is included in Eqn (2):

$$v_c \approx \frac{g\alpha a^2 T}{\nu} \approx \frac{\delta g\alpha a^4 I}{\nu\varkappa}, \qquad (16)$$

where g is the acceleration due to gravity. Steady thermal self-focusing is possible if the time τ_T for establishment of a steady temperature profile is less than the time $\tau_c = a/v_c$ for displacement of heated layers of a liquid across a beam. This criterion limits the intensity to

$$I < I_c = \frac{\eta\varkappa^2}{g\alpha\delta\rho_0^2 c_p a^5}. \qquad (17)$$

The value of I_c is 10^{-4} W cm^{-2} for benzene and 10^{-1} W cm^{-2} for glycerine, i.e. steady thermal self-focusing requires intensities $I \geqslant 1-10$ W cm^{-2}, attainable under transient conditions.

In the pulsed self-focusing regime the critical parameter is the energy $W_0 = \pi a^2 I_0 \tau$ [3]. It also determines the focal length of a nonlinear lens induced by sound. Therefore, the conditions for the observation of the self-focusing of sound should limit the pulse duration τ from below.

A thermal converging lens should be stronger than a diverging lens formed by flow:

$$v_x^0 < \frac{c_0|\gamma_p|T_0}{2} . \tag{18}$$

Substitution, in equality (18), of expressions (13) and (14) gives

$$\tau > \frac{a^2\rho_0 c_p}{c_0^2|\gamma_p|} \approx 1.3 \times 10^{-2}\,\mathrm{s} . \tag{19}$$

This means that flow does not stop heating throughout the interval $\tau = \tau_v$. In benzene the mechanism of flow activation is transient and, therefore, defocusing longitudinal flow does not mask self-focusing provided $A = c_p/c_0^2|\gamma_p| < 1$. Under normal conditions this parameter is $A = 0.14$ for benzene.

The self-focusing length should be less than the discontinuity length. The critical self-focusing energy W_{cr} can be found by equating L_f from expression (11) to the diffraction-spreading length L_s: $8|\Delta c|/c_0 = 0.61\lambda/a$. The velocity change Δc can be estimated by substituting expression (13) in Eqn (8). The result is

$$W_{cr} = \frac{(0.61)^2\pi\rho_0 c_p \lambda^2}{8|\gamma_p|\delta} , \tag{20}$$

For benzene this energy is 4 J and for glycerine it is 20 J.

The transient self-focusing length, estimated on the basis of Eqn (8) is

$$L_f = \frac{a^2(\pi\rho_0 c_p)^{1/2}}{2(|\gamma_p|\delta W_0)^{1/2}} . \tag{21}$$

For glycerine, when the intensity threshold is exceeded by a factor of 1.5, the value of L_f is less than 10 cm.

Finally, condition (4) and expression (21) set the limit on the pulse duration:

$$\tau > \tau^* = \frac{c_p(\varepsilon\omega a)^2}{|\gamma_p|\delta c_0^5} . \tag{22}$$

Here, the parameter τ^* determines the ratio of the effectiveness of the elastic and thermal nonlinear mechanisms.

The classical absorption mechanism (unrelated to the effects of molecular association) is characterised by $\delta \propto \omega^2$ and τ^* is frequency-independent. In the case of benzene we have $\tau^* = 3.6$ s and for glycerine, we have $\tau^* = 1.1$ s. This estimate forbids durations $\tau > \tau_v$.

The absolute rise in temperature can be estimated by substituting formula (20) into expression (13):

$$T = \left(\frac{0.61\lambda}{2a}\right)^2 \frac{W_0}{|\gamma_p|W_{cr}} . \tag{23}$$

For example, in the case of glycerine, we have $T = 1.7\,^\circ\mathrm{C}$ if $W_0/W_{cr} = 1.5$, i.e. dangerous overheating does not occur.

We shall now find the transient analogue of the criterion described by inequality (17), which excludes the influence of convection. If $\tau_v < \tau < \tau_T$, the velocity of sound-induced convection is estimated to be $v_c \approx 2g\alpha\delta W_0/\pi\eta c_p$. We shall require again that the time of convective motion across a beam ($\tau_c = a/v_c$) should be greater than the duration of an acoustic pulse τ when $W_0 = W_{cr}$:

$$\tau < \tau_c \approx \frac{10.8\eta|\gamma_p|a}{g\alpha\rho_0\lambda^2} . \tag{24}$$

For glycerine, we have $\tau_c = 10$ s. If $\tau < \tau_c$, the convection velocity is estimated to be $v_c = (2g\alpha\delta I_0\tau^2)/(\rho_0 c_p)$ and the condition for suppressing convection is

$$\tau < \left(\frac{a\rho_0 c_p}{2\delta g\alpha I_0}\right)^{1/3} , \tag{25}$$

An estimate based on inequality (25) shows that at the self-focusing threshold in benzene the process of convection destroys completely an acoustic beam in approximately 3.5 s.

It therefore follows that the thermal self-focusing effect can be observed in glycerine in the frequency range 1 – 10 MHz when the duration of the ultrasonic pulses is 1 – 10 s. In benzene, the self-focusing can be observed in the same frequency range, but the duration of insonation should be at least 3.5 s.

2.3 Self-induced transparency in an ultrasonic field

In Sections 2.1 and 2.2 we assumed that the dissipation parameters are constant and do not vary with the intensity of sound. However, strong temperature dependences of the acoustic absorption coefficient are typical of a number of liquids. Consequently, a change in the absorption coefficient of sound δ with increase in its intensity is possible in such liquids because of acoustic heating of the medium. Such changes should be particularly noticeable in liquids with strong intermolecular bonds which determine the dynamic short-range order. Bonds existing for a finite time in turn alter the acoustic spectrum of a liquid: sound builds

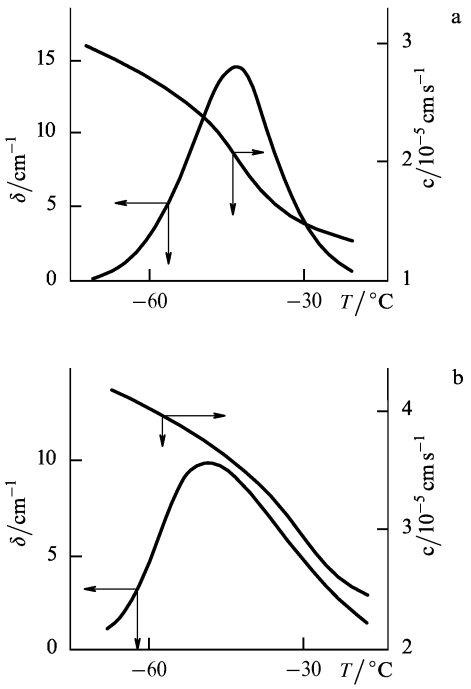

Figure 1. Temperature dependencies of the absorption coefficient δ and of the velocity of ultrasound c: (a) triacetin; (b) azeotropic aqueous solution of glycerine.

up what are known as relaxation oscillations, which are strongly damped because of the relative softness of the bonds, and wide absorption bands appear in the spectrum. The positions of these bands are influenced decisively by temperature because of their structural origin. For example, such behaviour has been observed in a megahertz frequency range for triacetin and an azeotropic aqueous solution of glycerine (Fig. 1): at temperatures from −70 °C to −20 °C a strong and monotonic variation of the velocity of sound $[\partial(\ln c)/\partial T \approx 10^{-2}\ \mathrm{K}^{-1}]$ is accompanied by a steep and nonmonotonic (passing through a maximum) change in the absorption coefficient $[\partial(\ln \delta)/\partial T \approx 10^{-2}\ \mathrm{K}^{-1}]$ [23]. In the range where $\partial\delta/\partial T < 0$, sound heats a medium and reduces the intrinsic absorption. An increase in the input intensity of sound increases the depth of its penetration into a medium and it is then natural to speak of the acoustic 'self-induced transparency'.

Let us assume that the conditions necessary for the self-focusing are satisfied. We shall seek a more general description of the self-action, including the self-induced transparency in the relaxation region. This requires that the dependence $\delta(T)$ should be added to the parabolic approximation equations. In our calculations, we shall assume that $\delta(T) = \delta_0 - (\partial\delta/\partial T)T^0$ ($\partial\delta/\partial T$ is a constant, T^0 will be simply denoted by T); therefore, the results obtained are valid if T is less than the width of the relaxation region ΔT_r. Subject to the limits considered above, the equations for T and $p = p^{\omega}$ deduced by reduction of the system of equations (1)–(3) become

$$(\partial_t - \chi\nabla_\perp^2)T = \frac{[\delta_0 - (\partial\delta/\partial T)\,T]|p^2|}{\rho_0 c_0 c_p}, \tag{26}$$

$$\left[\partial_x + c_0^{-1}\,\partial_t + \frac{\mathrm{i}\omega}{2c}\,\nabla_\perp^2\right]p = -\left(\delta_0 - \frac{\partial\delta}{\partial T}\,T\right)p + \mathrm{i}\,\frac{\omega}{c_0^2}\,\frac{\partial c}{\partial T}\,Tp\,. \tag{27}$$

We shall ignore thermal conductivity and assume that the thermal spreading time $\tau_T \geqslant 10^2$ s is no longer than the characteristic self-focusing and self-induced transparency times.

In the plane-wave limit, when the width of the input beam becomes $a \to \infty$ and the self-induced transparency occurs without self-focusing, the system of Eqns (26) and (27) reduces to [24]

$$\partial_u J = -\Theta J\,, \qquad \partial_v \Theta = \Theta J \tag{28}$$

for the functions

$$J = \frac{\partial\delta}{\partial T}\,\frac{I}{\rho_0 c_0 \delta_0 c_p}\,, \qquad \Theta = 1 - \frac{\partial\delta}{\partial T}\,\frac{T}{\delta_0}$$

and the variables are $u = \delta_0 x$, $v = \delta_0(c_0 t - x)$ subject to the boundary conditions

$$J(u = 0, v = \delta_0 c_0 t) = J_0(t)\,, \qquad \Theta(u = \delta_0 x, v = 0) = 1\,.$$

A second-order equation of the Liouville type follows from Eqn (28):

$$[\partial_{uv} + \exp(W\,\partial_u)]W = 0\,, \tag{29}$$

which applies to the function $W = \ln J$. The first integral of Eqn (29) gives the first-order equation for the function J^{-1}:

$$\partial_v J^{-1} + (J^{-1})^2 - f(v)J^{-1} = 0$$

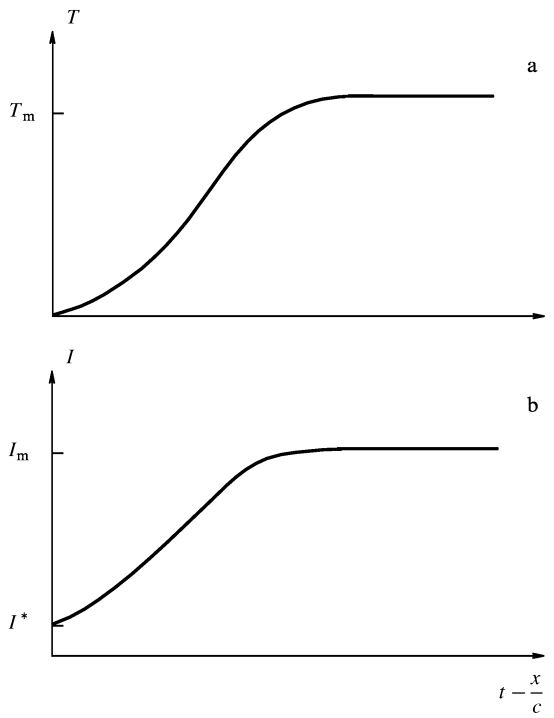

Figure 2. Transparency self-induced in the field of a plane wave: dependences of the temperature T (a) and of the intensity I (b) on the running time $t - x/c$ ($I^* = I_m \exp(-\delta_0 x)$, $T_m = \delta_0/|\partial\delta/\partial T|$).

[$f(v)$ is an arbitrary function]; the general solution of this equation is

$$J = \frac{J_0(v)\exp\left[\int_0^v J_0(t)\,\mathrm{d}t\right]}{\exp(u) + \exp\left[\int_0^v J_0(t)\,\mathrm{d}t\right] - 1}\,.$$

Fig. 2 gives the dependences $I(t)$ and $T(t)$ derived from Eqn (29) for a fixed distance x from a source; the input pulse is assumed to have the form of a step: $I_0(t < 0) = 0$, $I_0(t \geqslant 0) = I_0$. At the leading edge of a travelling pulse we have the usual absorption $I = I_0 \exp(-\delta_0 x)$, With time, the intensity increases if $\partial\delta/\partial T < 0$.

If a beam is of finite width and the paraxial approximation [3] is adopted, it is natural to seek the solution of the system of equations (26)–(27) for the specific case of a Gaussian profile of the input beam in the form

$$\begin{aligned} I &= I_0 J(t, x)\exp\left[-R(t, x)r^2\right], \\ -\frac{c_0}{\omega a^2 \delta_0}\arg p &= \varphi(t, x) + \tfrac{1}{2}\,\psi(t, x)r^2\,, \\ 1 - \frac{\partial\delta}{\partial T}\,\frac{T}{\delta_0} &= \Theta(t, x) + \tfrac{1}{2}\,\eta(t, x)r^2\,, \end{aligned} \tag{30}$$

where R, φ, ψ, Θ, η are the variable parameters of an ultrasonic beam. Here and later the transverse coordinate r is normalised to the beam radius a. Eqns (26) and (27) with the solution given by the set of expressions (30) lead to the following system of equations in terms of the coordinates u and v.

$$\begin{aligned} &\partial_u J + 2\psi J = -\Theta J\,, \quad \partial_u \psi + \psi^2 = -b_1 J + b_2 R^2\,, \\ &\partial_u R + 2\psi R = \frac{\eta}{2}\,, \quad \partial_v \Theta = -b_3 J\Theta\,, \\ &\partial_v \eta = -b_3 J\eta + 2b_3 J\Theta R\,, \quad \partial_u \varphi = b_1(1 - \Theta) - b_2 R\,. \end{aligned} \tag{31}$$

It follows that the effectiveness of a process is governed by three parameters b_1, b_2, b_3. Estimates of their values for glycerine at $T = -50$ °C are [in this range, the temperature derivative of the absorption coefficient is large: $(\partial \ln \delta/\partial T) \geqslant 0.1$ K^{-1}]:

$$b_1 = \frac{\partial c/\partial T}{(\partial\delta/\partial T)\delta_0 c_0 a^2},$$

$$b_2 = \left(\frac{\omega a^2}{\delta_0 c_0}\right)^{-2},$$

$$b_3 = \frac{(\partial\delta/\partial T)I_0}{\delta_0 \rho_0 c_p c_0}.$$

An approximate solution of the system of equations (31) can be obtained by iteration in which the diffraction effects are initially excluded ($b_2 = 0$). In this iteration method we start from the solutions of the system of equations (31), in which only the self-induced transparency is taken into account. The system can then be solved exactly [see Eqn (29)]. Substitution of these solutions into the system of equations (31) yields the Ricatti equation for the function ψ. The Ricatti equation can be solved by the WKB method on the assumption that

$$K = 2b_1 \xi \exp(\xi) > 1, \tag{32}$$

where

$$\xi = \frac{I_0|\partial\delta/\partial T|(t - x/c_0)}{\rho_0 c_p}.$$

For glycerine, we have $K = 2 \times 10^{-2} \xi \exp(\xi)$ and condition (32) excludes the range $\xi < 2.5$, whereas for viscous layers of finite thickness we have $\delta_0 x > 1$, so that we need to analyse only the case when $\xi > 1$ ($\xi \approx \delta_0 x$), since for small values of ξ the signal is close to zero: the process resulting in the self-induced transparency has not yet begun. The WKB integration demonstrates that the function Θ reaches the maximum value for $\xi = \xi_m \approx \delta_0 x - \ln(\delta_0 x)$. The intensity on the beam axis increases with the running coordinate ξ as long as the distance travelled in the liquid is $x < x_0$, where the length x_0 is found from

$$(2^5 b_1 \delta_0 x_0)^{1/2} \arctan\left[(\delta_0 x_0)^{1/2}\right] = \pi, \tag{33}$$

For glycerine, we have $x_0 \approx 1.5$ cm. Over longer distances ($x > x_0$), a pulse structure is formed; peaks ($J \to \infty$) appear at a denumerable number of points and the coordinates of these points satisfy the inequality $2b_1\xi > (2n-1)^2/4$. This inequality is stronger than that given by expression (32) and, consequently, the proposed theory predicts correctly the positions of the peaks of the functions J and R on the time scale.

The energy dependence of the self-focusing length $L_f = x_1$ on $W_0 = \pi a^2 I_0 t$ (in the absence of the self-induced transparency), given by expression (21), is of the falling type. Its minimum value is reached at

$$W = W^0 = \frac{\pi a^2 \rho_0 c_p \left[\delta_0 x_0 - \ln(\delta_0 x_0)\right]}{\partial\delta/\partial T} \approx 200 \text{ J}. \tag{34}$$

The final values of J and R at the peaks can be estimated if diffraction is taken into account. If we assume that $b_2 < 2b_1^2$ (estimates indicate that this assumption is justified in the case of glycerine), the second iteration of the system of equations (31) makes it possible to find a divergence-free solution by the WKB method and to calculate the peak values of the intensity, which are proportional to $16 b_1^2 J_p^0/\pi^2 (2n-1)^2 b_2$. For example, for glycerine at $T = -50$ °C at distances $x = 7.5$ cm from a source, an estimate of the intensity of the first peak gives $J(\xi = 15) \ll 1$ and that of the second peak is predicted to be $J(\xi = 62) \approx 3$. The relative beam radius $r = R^{-1/2}$ at a peak is 0.2, i.e. the beam is compressed by a factor of 5. The duration of the resultant pulse is estimated from

$$\Delta\xi = \frac{2\pi}{(2b_1\delta_0 x)^{1/2}} \approx 6. \tag{35}$$

If we go back to real time, t, we find that, for example, when the input intensity is $I_0 = 10$ W cm^{-2}, then 60 s after the activation of a source of sound a pulse of $\Delta t \approx 6$ s duration is formed and the intensity of this pulse is 3 times higher than that of the input pulse. The dependences of J on t and x obtained at the second iteration step are presented in Fig. 3.

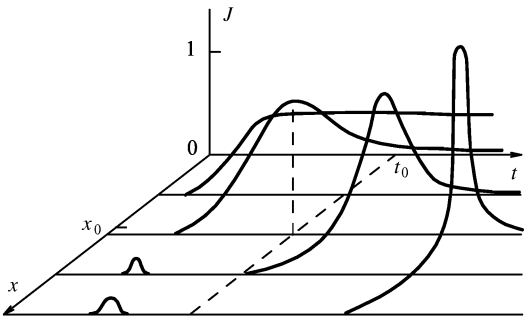

Figure 3. Self-focusing and self-induced transparency associated with an ultrasonic beam. The figure gives the dependence of the relative intensity J on the beam axis on time t and on distance x; $ct_0 = x_0 - \delta^{-1} \ln(\delta_0 x_0)$.

Separation of the self-focusing and self-induced transparency effects against the background of competing processes in a supercooled very viscous liquid is hindered only by heat conduction, because the development of flow is practically excluded. A steady-state temperature distribution is established in a beam in a time $\tau_T = a^2/\chi$. In our example, the beam radius decreases considerably at a peak and in estimating the values of τ_T we have to replace a with $a/R^{1/2} = a\pi(2n-1)b_2^{1/2}/4b_1$. The time for the appearance of the self-induced transparency is $t_{SIT} \approx \delta_0 x/b_3 c_0$ and, in order to exclude the influence of heat conduction, we must be sure to satisfy the inequality $t_{SIT} < \tau_T$. Hence, a limit is set on b_3 (and, consequently, on the input intensity I_0):

$$I > I_T = 16 b_1^2 \chi x \delta_0 \rho_0 c_p \left(b_2 \frac{\partial\delta}{\partial T}\right)^{-1} \left[a\pi(2n-1)\right]^{-2}, \tag{36}$$

In our example at a distance $x = 7.5$ cm, we have $I_T \geqslant 2-3$ W cm^{-2}. The precision of this estimate is limited because of the absence of information on the thermal diffusivity throughout the relevant temperature range.

2.4 Self-action of sound in a resonator

Investigations of the acoustic thermal self-focusing and self-induced transparency in viscous liquids have been continued in a natural manner in the resonator geometry [25]. The dependence $c(T)$ leads then to a shift of the normal frequencies of the resonator and to distributed feedback between the forward and reverse waves. Depend-

ing on the power of the exciting ultrasonic beam, various regimes of operation of the resonator are possible: they include bistable, self-oscillatory, and stochastic (the last represents irregular changes in the intensity of sound at the resonator exit).

A real ultrasonic beam has a finite aperture and the dispersive bistability leads to the appearance of inhomogeneities in the beam profile [26], so that the role of the effective beam radius under steady-state conditions is played by the size of its axial spot $a \approx k^{-1}$ (k is the wave number). In the case of a resonator of length l, filled with a liquid whose absorption coefficient is δ_0 and bounded by mirrors with the intensity reflection coefficients $R_1 = R_2 = R$ (one of the mirrors is the source of ultrasound of intensity I_i), it is reasonable to assume that the time taken to travel along the resonator is short ($l = 1$ cm, $t_r = l/c \approx 10^{-5}$ s), compared with the characteristic times analysed earlier.

The equation for describing the change in the acoustic pressure can be obtained from Eqns (1)–(3), (5):

$$\partial_{xx}^2 p + \left(\frac{\omega_0}{c_0}\right)^2 p = \mathrm{i}\,\frac{\omega_0}{c_0}\,\delta_0 p - 2\left(\frac{\omega_0}{c_0}\right)^2 \gamma_c T p\,. \tag{37}$$

where $\gamma_c = |\partial(\ln c)/\partial T|$. It is assumed that the length of formation of a shock wave exceeds l [see expression (4)]; moreover, the plane-wave approximation and the results of a numerical calculation [26] are sufficient. According to these results, the transverse effects (diffraction, self-focusing) in a bistable resonator reduce the effective beam radius.

For counterpropagating acoustic waves $p = p_f \exp(-\mathrm{i}kx) + p_b \exp(\mathrm{i}kx)$ and a temperature grating $T = T_0 + T_1 \exp(-2\mathrm{i}kx) + T_1^* \exp(2\mathrm{i}kx)$, it is found that Eqn (37) averaged over the spatial period $2\pi/k = 2\pi c_0/\omega_0$ together with the heat equation [deduced from Eqn (3)

$$\partial_t T - \chi \partial_{xx}^2 T + \frac{\chi}{a^2} T = \frac{\delta_0}{2\rho_0^2 c_p c_0} |p|^2 \tag{38}$$

on the assumption that the uniform temperature T_0 is affected mainly by diffusion in a transverse direction ($a < l$) and that the time for the establishement of T_0 exceeds the time for the establishment of T_1 ($2ka > 1$)], yield the following expressions in terms of partial derivatives [24] for six slow functions:

$$I_{f,b} = \frac{|p_{f,b}|^2}{2\rho_0 c_0 I_i}\,, \qquad \Phi = \arg(p_f) - \arg(p_b)\,,$$

$$\Theta_0 = T_0 \frac{2\omega_0 \gamma_c}{c_0}\,, \quad \Theta_1 = \frac{\omega_0 \gamma_c l}{c_0}\left[T_1 \exp(\mathrm{i}\Phi) + T_1^* \exp(-\mathrm{i}\Phi)\right],$$

$$\Theta_2 = \mathrm{i}\,\frac{\omega_0 \gamma_c l}{c_0}\left[T_1 \exp(\mathrm{i}\Phi) - T_1^* \exp(-\mathrm{i}\Phi)\right].$$

Let us introduce dimensionless variables $t' = t/\tau$, $x' = x/l$ (and then omit the primes) and write down the boundary conditions for them:

$$I_b(1, t) = b_1 I_f(1, t)\,,$$

$$1 = I_f(0, t) + b_1 I_b(0, t) - 2\left[b_1 I_b(0, t) I_f(0, t)\right]^{1/2} \cos\left[\Phi(1, t) + b_4\right], \tag{39}$$

$$\Phi(0, t) = \Theta_{0,1,2}(x, 0) = 0$$

The process is governed by five parameters:

$$b_1 = R\,, \qquad b_2 = \frac{2 I_i a^2 \delta_0 l \omega_0 \gamma_c}{\rho_0 c_p c_0 \chi} = \tilde{b}_2 I_i\,, \qquad b_3 = (2ka)^2$$

$$b_4 = 2(kl - \pi n)\,, \quad n \text{ is an integer}\,,$$

$$b_5 = \exp(-\delta_0 l)\,.$$

The parameters b_1 and b_5 govern the Q factor of the resonator, b_2 determines the resonator excitation power and the nonlinearity of the medium, b_3 governs the ratio of the times for the establishment of the uniform temperature T_0 and of the temperature grating T_1, and b_4 determines the detuning of the frequency of the incident ultrasound from the nearest normal resonator frequency ($0 < b_4 < 2\pi$). The dependence of the steady-state intensity of sound at the resonator exit $I_{out}^s = I_f(1)(1 - b_1) I_i$ on the input intensity, deduced from the above equations, is multivalued:

$$I_{out}^s = \frac{b_5 I_i (1 - b_1)}{1 + (b_1 b_5)^2 - 2 b_1 b_5 \cos\left[(2 + b_3^{-1}) \tilde{b}_2 I_{out}^s/(1 - b_1) + b_4\right]}. \tag{40}$$

If the resonator has a sufficiently high Q factor [$b_1 \approx 1$, $-\ln(b_5) < 1$], the intensities of the forward (I_f) and (I_b) counterpropagating waves are approximately equal ($I_f \approx I_b$) so that averaging over the resonator length leads to a system of ordinary differential equations for $\Theta_{1,2}(t) = \Theta_{1,2}(1, t)$ and $\Phi(t) = \Theta_0(t) + \Theta_1(t)$:

$$\begin{aligned} \dot{\Phi} &= \frac{3 b_2 J - \Phi - (b_3 - 1)\Theta_1}{1 - \Theta_2}\,, \\ \dot{\Theta}_1 &= -b_3 \Theta_1 + b_2 J + \dot{\Phi}\,\Theta_2\,, \\ \dot{\Theta}_2 &= -b_3 \Theta_2 - \dot{\Phi}\,\Theta_1\,, \end{aligned} \tag{41}$$

where $J = b_5 \exp(-\Theta_2)/[1 + (b_1 b_5)^2 - 2 b_1 b_5 \cos(\Phi + b_4)] = I_{out}^s/[I_i(1 - b_1)]$. The dot in the above system of equations denotes derivatives with respect to the dimensionless time t/τ.

Linearisation of the system of equations (41) in terms of small deviations from the steady-state values yields the characteristic equation:

$$\left(\frac{\lambda}{b_3}\right)^3 + \left(\frac{\lambda}{b_3}\right)^2 \left[1 + b_3^{-1} + 3P - 3Q\right] + \frac{\lambda}{b_3}\left[1 + 2b_3^{-1} + P(5 + b_3^{-1}) - Q(2 + b_3^{-1})\right] + P(2 + b_3^{-1}) + b_3^{-1} = 0\,, \tag{42}$$

where $P = -(b_2/b_3)(\mathrm{d}J/\mathrm{d}\Phi)$, $Q = (b_2 J/b_3)^2$, and the quantity $J = I_{out}^s/I_i(1 - b_1)$ is described by relationship (40). An analysis of the characteristic equation (42) shows that the self-oscillatory regime appears for $1 + b_3 + 3P - 3Q \approx 0$ and the period of self-oscillations $t_0 = 2\pi a^2/J[b_3(1 + 2Pb_3 + P)]^{1/2}$ increases with increase in the resonator length.

Numerical solution of the system of equations (41) makes it possible to study the stability of the steady-state solutions, to find the points of bifurcation of the appearance of a cycle, and study the solution near bifurcation points.

As the parameter b_3 increases, so does the number of the bifurcation points (Fig. 4): they appear in pairs and are shifted to the upper branches of the multistable dependence $\Phi^s(b_2)$. The lowest bifurcation point on the right shifts

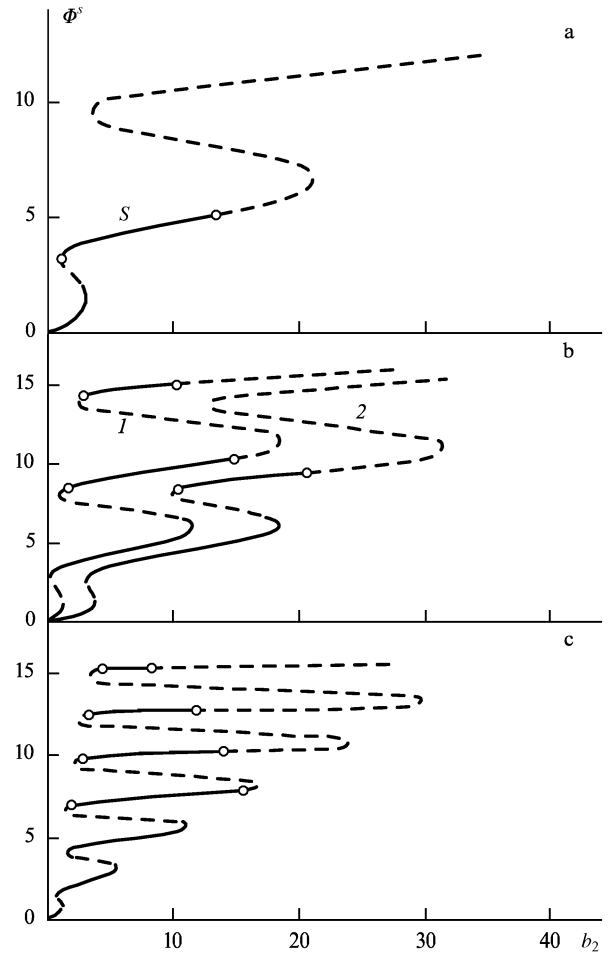

Figure 4. Bifurcation diagrams $\Phi(b_2)$, plotted for $b_1 = 0.9$, $b_4 = \pi$: (a) $b_3 = 2$, $b_5 = 0.6$; (b) $b_3 = 5$, $b_5 = 0.6$ (*1*) and 0.3 (*2*); (c) $b_3 = 10$, $b_5 = 0.6$. The continuous curves are the stable parts and the dashed curves are unstable.

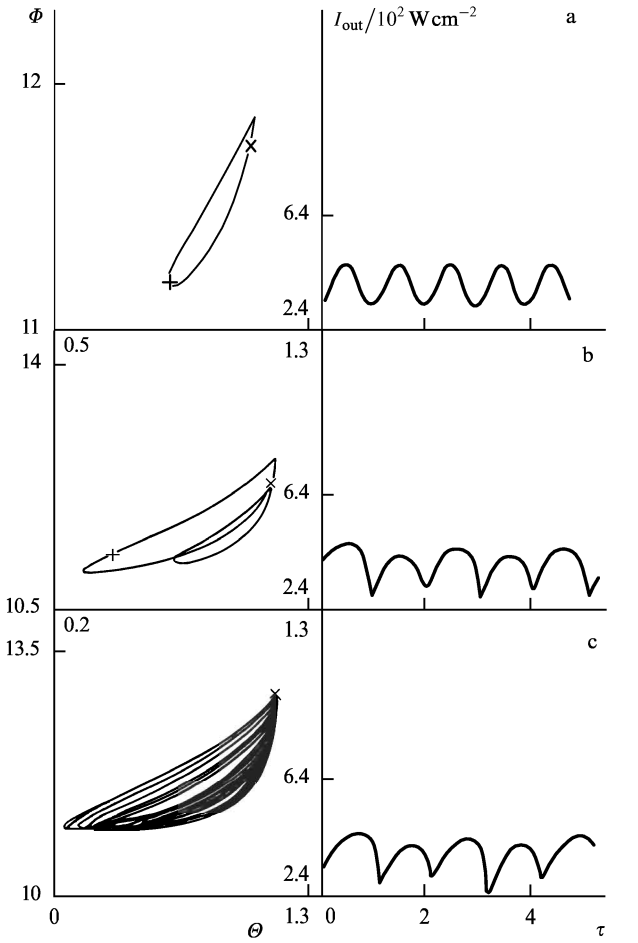

Figure 5. Phase diagrams $\Phi(\Theta_1)$ and the intensity of steady self-oscillations I_{out} $[\tau = t/(a^2/\chi)]$, plotted for $b_1 = 0.9$, $b_4 = \pi$, $b_5 = 5$: (a) $b_2 = 15.5$; (b) $b_2 = 16.5$; (c) $b_2 = 16.55$.

towards higher values of b_2. In the stability ranges the transmission assumes its steady value; the positions of the bifurcation points depend weakly on the detuning b_4. As b_5 is reduced (which happens with increase in $\delta_0 l$), the birfucation points on the upper parts of the dependence $\Phi^s(b_2)$ are suppressed and the lower right-hand bifurcation point shifts to the range of high values of b_2; the longer the resonator, the greater the value of I_i necessary in order to retain the self-oscillatory regime.

The single-period dependence $I_{out}(\tau)$ (Fig. 5a) experiences period doubling when crossing a bifurcation point (Fig. 5b). Then the sequence of period-doubling bifurcations leads to a stochastic regime in accordance with the Feigenbaum scenario (Fig. 5c).

3. Experiments

According to the theory presented above, there are quite definite and experimentally attainable conditions under which we can observe a transient thermal self-action of acoustic beams in liquid media of finite viscosity. This theory has been confirmed by a series of experiments [13, 17–19, 27–29] and all its main predictions, many of them stimulated by the first experiment [13], have been confirmed.

3.1 Self-focusing of an ultrasonic beam in a simple liquid

The first observation of the thermal self-focusing of ultrasonic beams in benzene, which has a relatively low viscosity, was reported in 1985 [13]. Benzene was enclosed in a cell (*1*) of 4 cm × 6 cm × 20 cm dimensions (Fig. 6). A ceramic disk (PZT-19 ceramic, 14 mm in diameter, resonance frequency 1.972 MHz) transducer (*2*) was built into one of the cell faces. At the opposite face there was a sound absorber in the form of Wood's horn

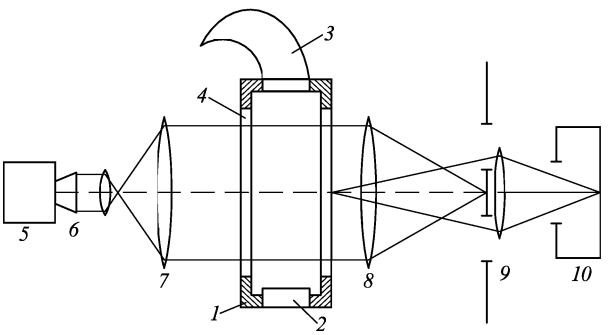

Figure 6. Schematic diagram of the apparatus: (*1*) cell; (*2*) ultrasonic transducer; (*3*) Wood's horn filled with an absorber; (*4*) optical windows; (*5*) laser; (*6–8*) optical lenses; (*9*) ring aperture; (*10*) photographic camera.

(*3*) filled with glass wool. The undesirable heating of the medium in the region of propagation of the acoustic beam by the heat released during the operation of the transducer was prevented by placing, in front of the transducer, a three-layer thermal filter made of a polytetrafluoroethylene film 50 μm thick. The cell had side windows (*4*) made of optical glass for illumination of the liquid with laser radiation. The source of this radiation (*5*) was either the cw He–Ne laser (emission wavelength $\lambda = 0.63$ μm, output power $P = 10$ mW) or a pulsed Nd^{3+}:YAG laser with frequency doubling in an $LiNbO_3$ crystal ($\lambda = 0.53$ μm, pulse duration $\tau = 15$ ns, energy $E = 3$ mJ). The duration of the laser pulses was much less than the acoustic wave period.

During continuous illumination the field of an image of the ultrasonic beam consisted, because of the Raman–Nath diffraction, of alternate dark and bright fringes, which were the result of pure phase modulation. Such modulation was retained to sound intensities of 10^2 W cm^2. In the experiments reported in Refs [13, 17–19, 28, 29] an aperture (*9*), placed in front of a photographic camera, transmitted only the zeroth diffraction order, in accordance with the 'bright field' method. The 'bright field' pattern was formed by an optical system comprising lenses (*6–8*), the aperture (*9*) and the photographic camera (*10*). This method enabled us to measure the geometric size of the beam (from the change in the distance between the diffraction pattern fringes) and the total power in a selected section of the medium (from the number of the diffraction fringes). Illumination of a travelling acoustic wave with pulsed laser radiation made it possible to observe also the phase fronts of the acoustic beam and, con- sequently, to determine more accurately the boundaries of the beam.

These experiments [13, 17–19, 28, 29] were carried out after a preliminary calibration of the transducers and receivers. The piezoelectric ceramic transducer was excited by a voltage supplied from a stabilised hf oscillator with a power amplifier, so that the acoustic power carried out by the beam could be up to 50 W. Under these conditions the thermal self-focusing mechanism in benzene should, in accordance with Section 2.2, be only transient. When the duration of insonation τ was less then $\tau_v \approx 10$ s and the time for the establishment of the uniform temperature was $\tau_T \approx 10^2$ s. the defocusing longitudinal flow and heat conduction were inactive provided $A = c_p/c_0^2\gamma_p < 1$. This requirement was satisfied for benzene: $A = 0.14$. Under the conditions in Refs [13, 29] the sound-induced convection was also transient and did not destroy the beam provided $\tau < \tau_c = 1.4$ s. Multistage generation of harmonics could be suppressed completely for $\tau > \tau_p \approx 39.5$ s. For $\tau > \tau_p$, the harmonics were generated but the process was not too advanced (a shock was not inverted), which did not prevent self-focusing but simply caused distortions in the transverse distribution of the intensity in the acoustic beam and reduced somewhat the self-focusing threshold estimated, in accordance with expression (20), to be $W_{cr} \approx 3.9$ J.

Control experiments were carried out on water with a positive temperature derivative of the velocity of sound right up to $T \approx 74.5$ °C. Consequently, self-focusing of sound was in principle impossible. In fact, when the power in the beam was $P \approx 50$ W, no changes were found in the beam profile over a period $\tau \approx 10$ s.

The first experiments on benzene [13] showed that a significant increase in the temperature of the medium in the region of an acoustic beam resulted from the heat flux released by the transducer. Such heating made the medium turbulent and distorted considerably the wavefront of the acoustic beam, which prevented self-focusing. This heat flux was excluded by placing a number of thermal filters, perpendicular to the direction of propagation of the beam and made of a polytetrafluoroethylene film 50 μm thick. In control experiments these filters were located at distances of 2.5 cm from the transducer and from one another and they did not prevent ultrasound propagation. However, they reduced considerably the penetration of heat released by the transducer. In all the subsequent experiments we used just one multilayer thermal filter located near the transducer.

An analysis of the results of optical visualisation of an acoustic beam in benzene with the aid of cw He–Ne laser radiation showed that the change in the beam cross section became significant when the acoustic energy reached $W \approx 2$ J ($P = 20$ W). The main changes were beam contraction and reduction in the distance between the fringes in the diffraction pattern (Fig. 7). The boundaries of the contracted beam were clearly visible. Spreading of the fringe in the upper and lower parts of the images corresponded to the side lobes of the emission diagram

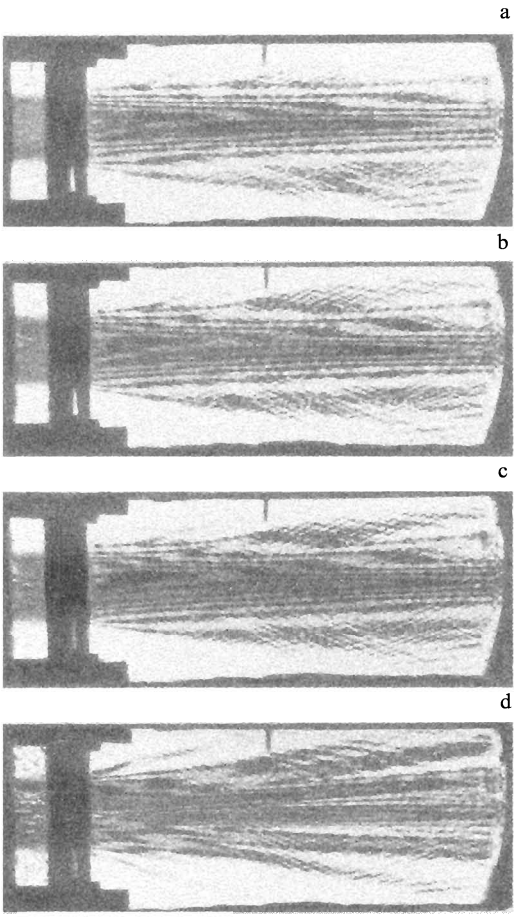

Figure 7. 'Shadow' patterns of the distribution of the intensity of an acoustic beam in benzene. The input acoustic radiation power was $P = 15$ W and patterns were recorded at the following times after activation of the source: (a) 0.2 s; (b) 0.5 s; (c) 1 s; (d) 2 s. The transducer source was located on the left and the heat filter can be seen.

of the acoustic transducer and to reflections from the cell walls.

An increase in the acoustic energy at constant power delivered to the transducer resulted in motion of the beam waist, which then formed, towards the transducer. The velocity of the beam waist or, in other words, the change in the self-focusing length L_f agreed with the theoretical predictions given in Section 2.2: for $P = 15$ W, we found (for example) that $L_f = 8.8t^{-1/2}$. When the acoustic beam energy was increased to $W \approx 30$ J, the beam contracted by a factor exceeding 2. A further increase in this energy broke up the acoustic beam into several filaments (nonlinear aberration) at angles to the axis. These filaments carried an energy of the order of the critical value, as deduced from estimates from the frequencies of the fringes in the 'shadow' pattern. The acoustic power in the beam was determined from the number of alternate 'bright' fringes inside the beam [30] and the results were compared with those produced by probe measurements.

Visualisation of the ultrasonic beam in benzene with the aid of pulsed Nd^{3+}:YAG laser radiation showed [29] how the radius of curvature of the wavefronts changes (Fig. 8). An increase in the acoustic energy at the beam centre, where heating was stronger, delayed the wavefront relative to the beam periphery. When the delay reached $\lambda/2$ (half the distance between the dark fringes in Fig. 8), the front broke up and the main beam split into several components.

Measurements of the radius of curvature of the wavefronts gave a fairly accurate value of the self-focusing length L_f, representing the position of the waist where the sign of the radius of curvature was reversed and the radius became infinite. When the acoustic energy was $W \approx 150$ J, the self-focusing length L_f was approximately 10 cm [29].

3.2 Self-focusing and self-induced transparency in a high-viscosity liquid

A natural development of the work reported in Refs [13, 29] was the investigation of the mechanisms of the thermal self-interaction of ultrasound in viscous liquids [17–19, 29, 31]. The bulk of the experiments on, for example, glycerine [17, 29] was carried out with apparatus similar to that shown in Fig. 6. Glycerine was selected because, even at room temperature, its viscosity η and the absorption coefficient of sound δ are considerably greater than those of benzene; moreover, the negative temperature derivative of the absorption coefficient of glycerine, amounting to $\partial(\ln\delta)/\partial T \approx -0.07$ K^{-1}, is also greater. The duration of observation t of the self-action effects satisfied now different conditions: $\tau_T \gg t \gg \tau_v$, where $\tau_T \approx 5 \times 10^2$ s and $\tau_v \approx 5 \times 10^{-2}$ s for $a = 0.75$ cm. Under these conditions the sound-induced convection was quasisteady and its velocity $v_c \approx 2g\alpha\delta Pt/\pi\eta c_p$ was so low (because of the high viscosity η) that the influence of the convection on self-focusing was practically negligible.

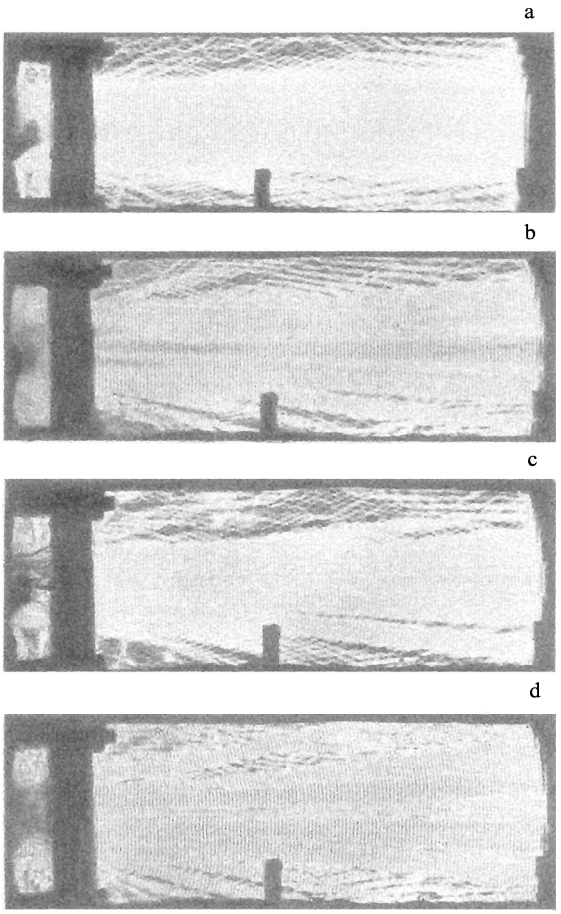

Figure 8. Patterns showing the distribution of the intensity of an acoustic beam ($P_0 = 20$ W) in benzene, recorded by illumination with pulsed laser radiation at the following moments: (a) 0.1 s; (b) 0.5 s; (c) 1 s; (d) 1.5 s.

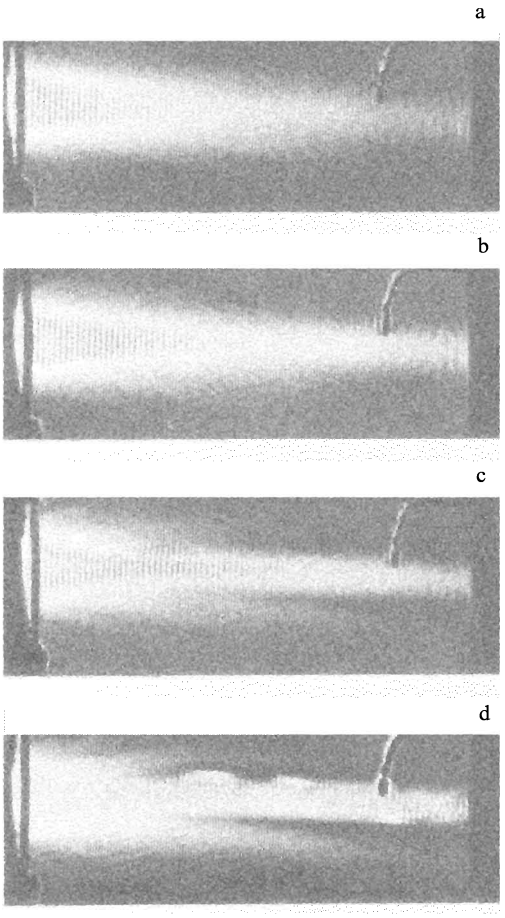

Figure 9. Patterns showing the distribution of the intensity of an acoustic beam ($P_0 = 8$ W) in glycerine (pulsed laser illumination): (a) 0.1 s; (b) 5 s; (c) 10 s; (d) 15 s.

Condition (25), which had to be satisfied to justify such neglect, was obeyed.

According to an estimate represented by inequality (22), the generation of higher harmonics could be ignored if $t \geqslant 1$ s. In fact, when the injected acoustic energy exceeded by a factor of 1.5–4 the critical self-focusing energy amounting to 20 J, the irregularity of the shadow patterns remained undisturbed for hundreds of seconds.

In addition to optical detection, we carried out also probe measurements of the temperature and pressure distributions in an acoustic beam. Both optical and probe measurements showed that an increase in the injected acoustic energy W caused contraction of the beam which could reach a factor of 2 at $W = 800$ J. A detailed pattern of this contraction mechanism was provided by optical measurements: the phase fronts of sound in the region adjoining the transducer had a negative curvature and far from it they had a positive curvature. Therefore, an acoustic beam formed a converging thermal lens (Fig. 9) in glycerine and benzene.

Since glycerine had a high temperature derivative of δ, the thermal self-induced transparency could be observed for the first time: the depth of penetration of an acoustic beam into glycerine increased with increase in the injected energy: the effective penetration depth L was 5.5, 6.7, and 7.9 cm for $W \approx 7$, 40, and 80 J [17].

The relative effectiveness of the self-focusing and self-induced transparency processes was described by the parameter b_1, introduced in Section 2.3 and equal to the energy needed to make the liquid transparent to sound over a distance x (equal to the diffraction spreading length L_s), divided by the critical self-focusing energy. In room-temperature experiments on glycerine it was found that $b_1 = 12.5$ and, therefore, the self-focusing predominated over the self-induced transparency.

Probe measurements of the pressure and temperature on the acoustic beam axis and at its periphery (Fig. 10) gave estimates of the times in which quasisteady levels of the sound-induced changes in these quantities were established.

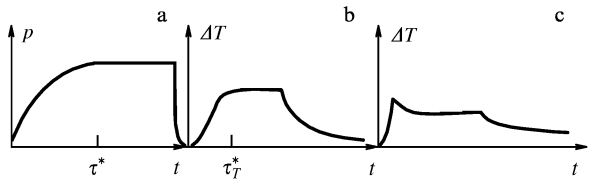

Figure 10. Time dependences of the pressure and temperature in glycerine at a distance of 7.5 cm from the transducer: (a, b) on the beam axis; (c) on the beam periphery.

3.3 Self-action of ultrasound in the relaxation absorption range

It was demonstrated in Sections 2.2 and 2.3 that the use of viscous liquids makes it possible to increase the time scale of experiments and to ensure injection of a higher acoustic energy at a given level of the input power. Moreover, in a detailed investigation of the self-action effects it is desirable to vary a number of parameters of the medium (δ, $\partial\delta/\partial T$, $\partial c/\partial T$) in the widest possible range of values. It was found that this is possible in the case of quasistructural high-viscosity liquids and that the temperature dependence of the absorption was strongly dome-shaped (see Fig. 1). For example, an increase in temperature of an aqueous solution of glycerine and of triacetin from −80 °C to +20 °C increased the absorption coefficient δ of ultrasound from 10^{-2} to 15 cm^{-1} and the temperature derivative of this coefficient was ± 1 cm^{-1} K^{-1} [23]. The values of the derivative $\partial c/\partial T$, which govern the effectiveness of the self-focusing process, varied from −2 to −40 m s^{-1} K^{-1}. Experiments on an aqueous solution of glycerine (with 13% of water) and on triacetin were carried out with modified apparatus. A massive stainless-steel cell was of rectangular shape and its dimensions were 20 cm × 6 cm × 4 cm. Its thermal insulation was improved by providing it with double optical windows (20 cm × 4 cm). The other surfaces of the cell were also double and the space between the walls was used to circulate a cooling agent. These experiments were carried out over the whole temperature range from −80 °C to +20 °C employing a system for thermal stabilisation and cooling with liquid or gaseous nitrogen. The cell was fitted with additional external heat exchangers with highly branched internal channels. The required temperature and its uniform distribution over the cell volume were maintained with an error not exceeding 0.1 °C. The temperature relaxation time of the medium after interaction with an acoustic beam ranged from 15 min to 3 h.

The temperature dependences of the absorption and velocity of ultrasound in triacetin (Fig. 11) and also in an aqueous solution of glycerine could be divided into five characteristic ranges. The results of an investigation in each of these ranges are of intrinsic interest.

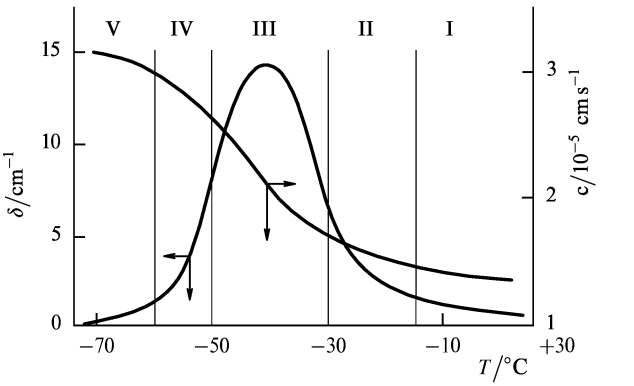

Figure 11. Characteristic ranges in the temperature dependences of the ultrasonic parameters (absorption coefficient and velocity) of triacetin.

I. T_0 = –15 °C to 20 °C

The absorption is weak: $\delta \leqslant 0.05$ cm^{-1}; the temperature derivatives of the absorption coefficient and the velocity of sound are low: $\partial\delta/\partial T \approx 0.1$ cm^{-1} K^{-1} and $\partial c/\partial T = -(3-6)$ m s^{-1} K^{-1}; the viscosity is $\eta = 0.1-5$ P. The self-focusing process predominates in both liquids. However, this process is not very effective: in view of the low viscosity, the growth time of the process is limited in the absence of competing processes. The experimental results for this temperature range in fact repeat the data obtained for benzene [17]. The time dependence of the pressure of sound on the beam axis, typical of the temperature range I, is shown in Fig. 12a.

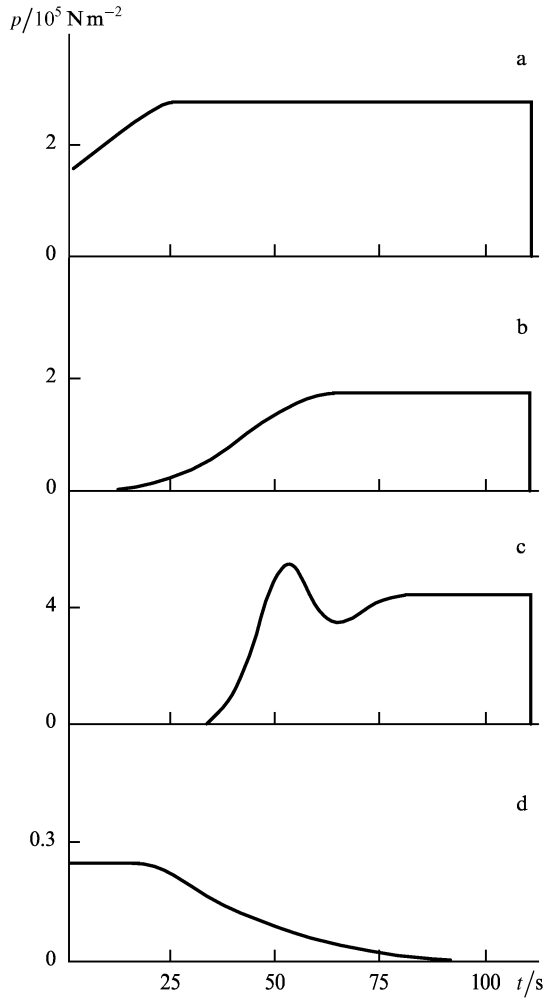

Figure 12. Time dependences of the pressure of ultrasound in triacetin on the the beam axis at 5 cm from the transducer, determined for different initial temperatures and intensities; (a) $I_0 = 2$ W cm^{-2}, $T_0 = 20$ °C; (b) $I_0 = 2$ W cm^{-2}, $T_0 = -25$ °C; (c) $I_0 = 3$ W cm^{-2}, $T_0 = -40$ °C; (d) $I_0 = 3$ W cm^{-2}, $T_0 = -65$ °C.

II. T_0 = –30 °C to –15 °C

The absorption in this range is fairly strong ($\delta = 1-7$ cm^{-1}). The high viscosity ($\eta = 10^2-10^3$ P) and the large negative temperature coefficients ($\partial\delta/\partial T \approx -10^{-1}$ cm^{-1} K^{-1}, $\partial c/\partial t = -(4-15)$ m s^{-1} K^{-1}) ensure that ultrasound penetrates the investigated medium to distances at which significant changes occur in the transverse size of the acoustic beam. The self-focusing develops solely because of the self-induced transparency, so that the establishment of an acoustic pressure in the medium is delayed and the delay is represented by the time taken by the self-induced transparency to develop (Fig. 12b).

III. T_0 = –50 °C to –30 °C

The maximum absorption ($\delta \geqslant 10$ cm^{-1}), the large negative derivative $\partial c/\partial T \approx -40$ m s^{-1} K^{-1}, and the values of $\partial\delta/\partial T$ ranging from -1 to $+1$ m s^{-1} K^{-1} make it possible to inject a high acoustic energy into the medium and to attain the self-induced transparency even when its threshold is high (about 100 J), but this happens only close to the transducer ($x < 2.5$ cm). Therefore, as indicated by estimates given in Section 2.3, pure self-focusing is not observed. On the other hand, a strong temperature dependence of the velocity of sound makes it possible to identify clearly the self-focusing process which develops after self-induced transparency. The time dependence of the acoustic pressure has a characteristic pulse-like signal peak, which is the result of self-focusing and represents formation as well as motion of a thermal lens against the background of monotonic growth of the self-induced transparency (Fig. 12c). In this temperature range the initial position on the absorption curve (to the right or left of the maximum) affects only the self-induced transparency time.

IV. T_0 = –60 °C to –50 °C

In this case the high absorption coefficient ($\delta \approx 1-5$ cm^{-1}), the positive derivative $\partial\delta/\partial T > 0$, and the negative derivative $\partial c/\partial T \approx -(30-40)$ m s^{-1} K^{-1} represent a set of parameters of the medium which are of no great interest: ultrasound penetrates a liquid to a depth not exceeding 1 cm.

V. T_0 < –60 °C

The absorption coefficient $\delta \approx 0.1-0.5$ cm^{-1}, the positive derivative $\partial\delta/\partial T > 0$, and the negative derivative $\partial c/\partial T = -10$ m s^{-1} K^{-1} ensure 'self-darkening', which is a reduction in the depth of penetration of an ultrasonic beam when its intensity is increased (Fig. 12d).

The greatest interest lies in the ranges of maximum absorption (II and III) of ultrasound, corresponding to $\delta(-50\ °C) \approx 10$ cm^{-1} for glycerine (see Fig. 1).

At low values of the input intensity, $I < I_T$ [defined by inequality (36)], when the influence of the thermal conductivity is significant, the temperature in the paraxial region of the beam remains low, and the effectiveness of the self-interaction is low. In fact, if the input intensity of sound is of the order of 2 W cm^{-2} (Fig. 13a), the experimental results are in qualitative agreement with the estimates given in Section 2.3, but the intensity of sound on the beam axis is less than that predicted theoretically.

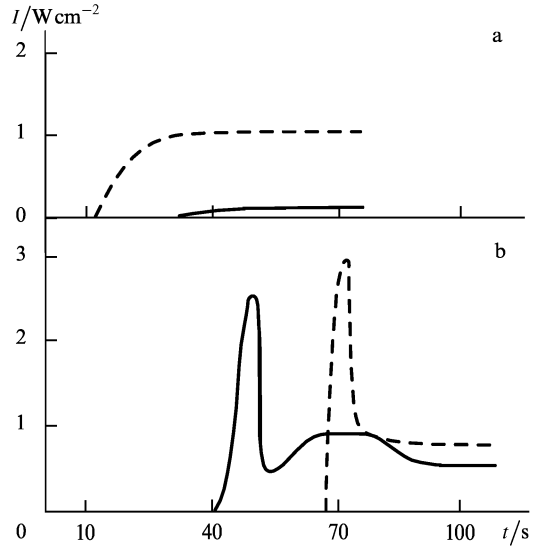

Figure 13. Time dependences of the intensity of ultrasound in glycerine (initial temperature $T_0 = -43$ °C) measured on the beam axis at a distance of 7.5 cm from the transducer: (a) $I_0 = 2$ W cm^{-2}, (b) $I_0 = 8$ W cm^{-2} (the continuous curves are experimental and the dashed curves are calculated).

An increase in the input intensity of the acoustic beam to $I_0 > I_T$ reduces considerably the times needed for the development of the self-focusing and the self-induced tranparency, so that the thermal conductivity becomes unimportant. When the intensity is $I_0 = 8$ W cm^{-2}, strong self-concentration of the acoustic energy both in space and time is observed in a liquid at a distance $x = 7.5$ cm from the transducer: a pulse of $\Delta t = 8$ s duration is formed and the peak intensity in this pulse is over twice as high as the input intensity of sound I_0 (Fig. 13b). Theoretical estimates agree well with the experimental data. However, it should be pointed out that measurements of the acoustic wave intensity are subject to an error of approximately 50%, whereas the time scale of the process is inversely proportional to the intensity. A significant influence of the self-induced transparency on the observed pattern is confirmed quite definitely: an increase in the injected energy displaces the focus of a nonlinear lens away from the transducer and not towards it, in contrast to the self-focusing in the absence of the self-induced transparency.

The dependences of the effectiveness of nonlinear processes on the initial intensity of sound were investigated throughout the whole relaxation temperature range also for triacetin, which is a medium with a maximum of the absorption of ultrasound: $\delta(-41\ ^\circ\text{C}) = 14$ cm^{-1} [18].

At the highest temperatures (range I), the self-focusing occurred at intensities limited from below by the thermal conductivity and induced flow and from above by the generation of harmonics: for glycerine the limits were $1 \leqslant I \leqslant 8$ W cm^{-2} (Fig. 14a) and for the triacetin, the corresponding limits were $0.3 \leqslant I \leqslant 3$ W cm^{-2}. The radius of the acoustic beam in the focal waist region reached 0.3–0.4 cm and the intensity was a factor of 2–2.5 higher than the input value.

The experimental threshold for the observation of the self-induced transparency at somewhat lower temperatures (range II) was 1 W cm^{-2} for glycerine and 0.5 W cm^{-2} for triacetin. The maximum depth of penetration of an acoustic beam was 10–15 cm for glycerine at $I = 8$ W cm^{-2} and for triacetin at $I = 5$ W cm^{-2} (Fig. 14b). At higher intensities the beam was destroyed by the sound-induced flow.

In the region of the absorption maximum (range III), the threshold for the observation of the self-induced transparency in these liquids rose to 1.5 and 1.3 W cm^{-2}, respectively. When the initial temperature was in the vicinity of the absorption maximum and the

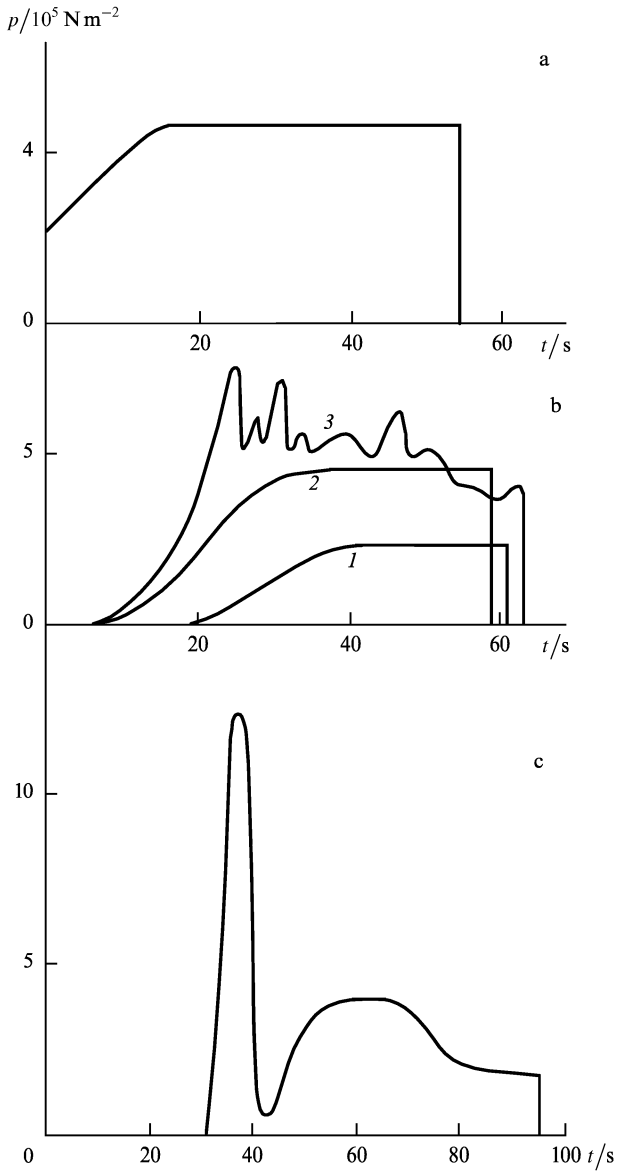

Figure 14. Time dependences of the pressure of ultrasound in glycerine measured on the beam axis at a distance of 5 cm from the transducer: (a) $T_0 = 20\ ^\circ$C, $I_0 = 4$ W cm^{-2}; (b) $T_0 = -30\ ^\circ$C, $I_0 = 5$ W cm^{-2} (*1*), $I_0 = 8$ W cm^{-2} (*2*), $I_0 = 10$ W cm^{-2} (*3*); (c) $T_0 = -48\ ^\circ$C, $I_0 = 8$ W cm^{-2} (at $x = 7.5$ cm).

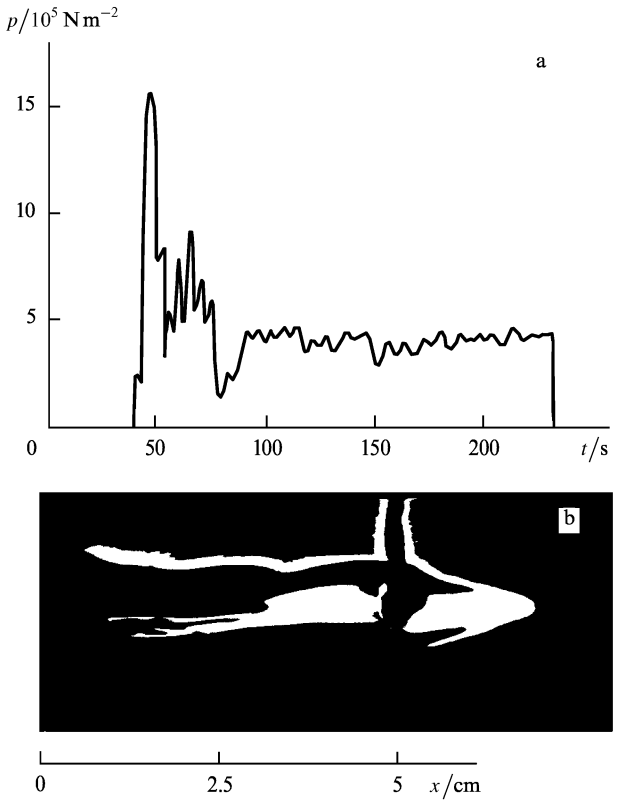

Figure 15. Self-concentration of an acoustic beam in glycerine observed for $I_0 = 8$ W cm^{-2} and $T_0 = -48\ ^\circ$C: (a) time dependence of the pressure on the beam axis at $x = 7.5$ cm; (b) optical image of the intensity distribution in the focal region recorded 30 s after activation of the transducer source.

input intensity was near the threshold of flow ($I \approx 10$ W cm^{-2}), the simultaneous effect of spatial and temporal self-concentration of the acoustic energy was the most striking effect; this looks promising for practical applications (Fig. 14c). At distances of several centimetres from the transducer an acoustic pulse reached its peak intensity which was several times higher than the input value I_0. Probe (Fig. 15a) and optical (Fig. 15b) measurements demonstrated that the transverse size of the focal region was then 2–3 wavelengths and its longitudinal size did not exceed 5–7 wavelengths.

Selection of the optimal values of the parameters (observation distance $x = 7.5$ cm, initial temperature $T_0 = -54$ °C, and input ultrasonic wave intensity $I_0 = 10$ W cm^{-2}) maximised the enhancement of the intensity of ultrasound to more than one order of magnitude, compared with the initial value (Fig. 16). In the focal region the beam had sharp boundaries: at a distance of 2–3 mm from the beam axis it was not possible to detect the ultrasonic field (the sensitivity threshold of the apparatus was 10^{-3} W cm^{-2}). The intensity in the beam waist was sufficiently high to generate a shock wave: when self-concentration occurred at short distances from the transducer, the spectrum of the ultrasonic wave became enriched with higher (up to the fourth inclusive) harmonics. According to the estimates in Section 2.3, the intensity at the focus at a distance of 7.5 cm should be 100–150 W cm^{-2}. Probe measurements gave a value not exceeding 60 W cm^{-2}, which could be explained partly by the narrow-band nature of the detector. The time taken to induce the transparency was 50 s, the duration of an acoustic pulse formed in this way was 5 s, and the smallest size of the region of localisation of the self-concentrated ultrasound was 5–7 mm. The bulk of the beam power was therefore concentrated in the volume $10^2\lambda^3 = (2-6) \times 10^{-2}$ cm^3.

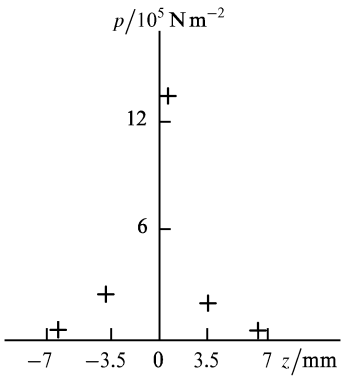

Figure 16. Pressure distribution in a transverse section of the beam at a distance of 7.5 cm from the transducer, recorded 45 s after activation of the transducer under conditions of self-concentration of the ultrasonic beam in glycerine at $T_0 = -54$ °C for $I_0 = 10$ W cm^{-2}.

The self-darkening effect was observed (Fig. 17a) at the lowest temperature (range V) for input intensities $I_0 > 0.05$ W cm^{-2}. The ultrasonic wave intensity changed by several orders of magnitude. As expected, the self-darkening effect developed faster in the acoustic beam axis. When the initial intensity of the ultrasonic beam was increased by an order of magnitude or more (to 0.5–1 W cm^{-2}), the dependences of the acoustic pressure in the interior of the medium ceased to

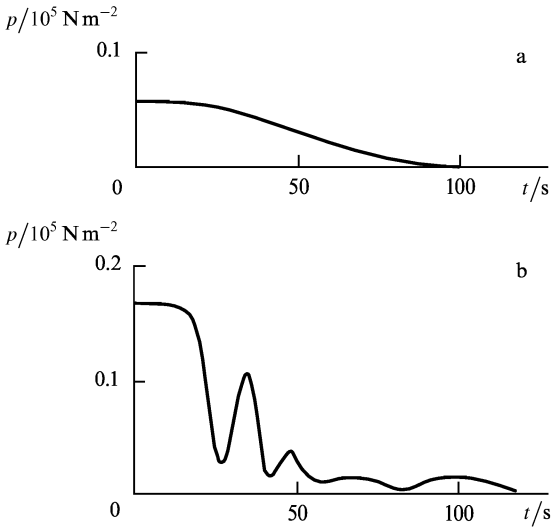

Figure 17. Time dependences of the pressure of ultrasound in glycerine recorded at 5 cm from the transducer under self-darkening conditions: (a) $T_0 = -65$ °C, $I_0 = 0.1$ W cm^{-2}; (b) $T_0 = -64$ °C, $I_0 = 0.3$ W cm^{-2}.

be monotonic and oscillations with a period of 10–30 s, depending on the initial conditions, were observed against the background of the decaying signal (Fig. 17b). Such an oscillatory regime could be attributed to the simultaneous (and mutual) influence of heat conduction, self-darkening, and self-focusing processes.

An approximate WKB theory of the self-action of wave packets (Section 2.3) predicted [31] a moving multifocus (at high input intensities of ultrasound) structure of the field in a liquid. Refinement of this theory by a numerical experiment [32] ensured, first, a practically complete quantitative agreement with the results of an investigation of the time dependence of self-concentration (Figs 18a,

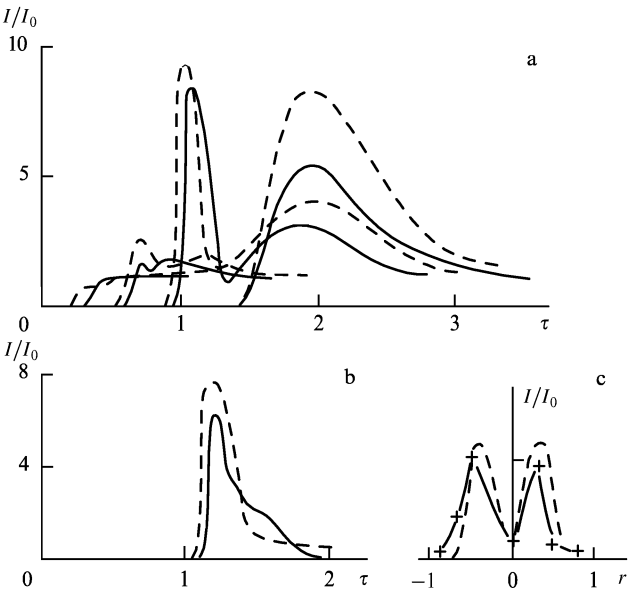

Figure 18. Dependences of the relative intensity of ultrasound on the beam axis: (a) on time (formation of two pressure pulses; (b and c) on time and on the transverse coordinate, respectively, when focusing produced a ring-shaped pattern. The continuous curves are experimental [19] and the dashed curves are calculated [32].

18b). Second, this refinement demonstrated that when the threshold was exceeded, the transverse structure of the beam could change not only quantitatively but also qualitatively: 'a silent zone' appeared at the centre of the acoustic beam and the beam was focused to form a ring (Fig. 18c). These predictions were supported fully by the experimental results [18, 32] obtained for viscous liquids (glycerine and triacetin): an increase in the injected ultrasonic energy gave rise to several 'hot spots' in a medium (Figs 18a and 19b) and the acoustic energy was transferred to a peripheral ring-shaped zone (Figs 18c, 19c). The parameters of the curves in Fig. 19 were $\omega^2 a^2 |\partial c/\partial T|/c_0^3 |\partial\delta/\partial T| = 4$, $\omega a^2 \delta_0 c_0 = 130$, $\omega a^2 |\partial\delta/\partial T| I_0/\rho_0 c_0 c_p = 1.75 \times 10^{-5}$.

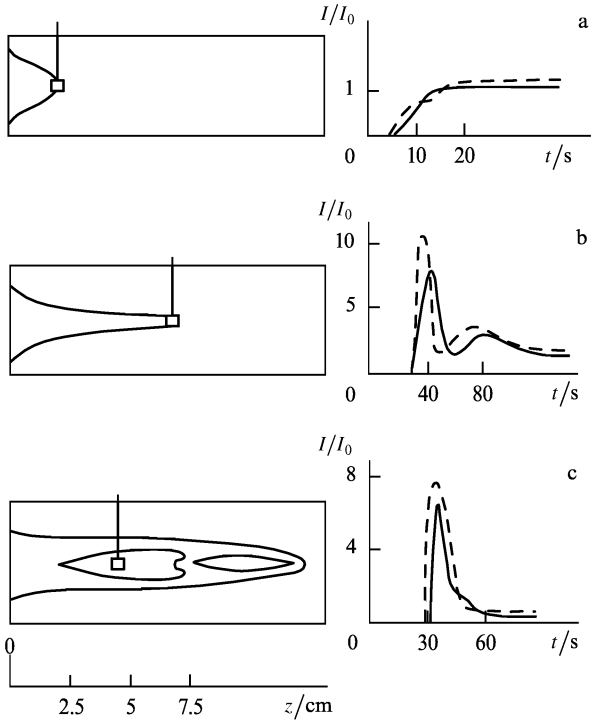

Figure 19. Equidensity lines in an optical image of an ultrasonic beam at the following moments: (a) 10 s; (b) 30 s; (c) 80 s. The time dependences of relative intensity, obtained at the positions of the sensor in these images, are plotted on the right: the continuous curves are experimental and the dashed curves are calculated.

3.4 Nonlinear thermal effects in an acoustic resonator

Nonlinear processes in a resonator (cavity) containing a medium with nonlinear optical properties have been investigated in detail, both theoretically and experimentally [33]. Bistability of an optical resonator makes it possible to use it, depending on the nature of the nonlinearity and on the feedback mechanism, as an optical limiter, a differential amplifier, an optical transistor, and a memory device.

Nonlinear acoustic resonators have been investigated much less. Measurements of the frequency shift of the modes in a resonator placed inside a cell containing glycerine, caused by a change in the velocity of sound as a result of sound-induced heating of a medium, was measured [25]. The shift of the mode centre was determined and it was found that this shift exhibited a hysteresis at sufficiently high intensities of ultrasound.

Detailed investigations of various regimes of ultrasonic self-oscillations in a nonlinear resonator are reported in Refs [25, 27]. The experiments described there were a continuation of investigations of the thermal self-focusing

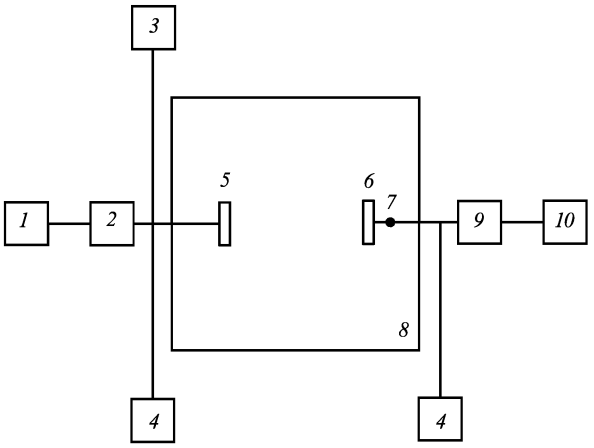

Figure 20. Schematic diagram of the apparatus: (*1*) oscillator; (*2*) amplifier; (*3*) frequency meter; (*4*) oscilloscope; (*5*) transducer; (*6*) mirror; (*7*) piezoelectric transducer (detector); (*8*) thermally stabilised cell with glycerine; (*9*) voltmeter; (*10*) automatic plotter.

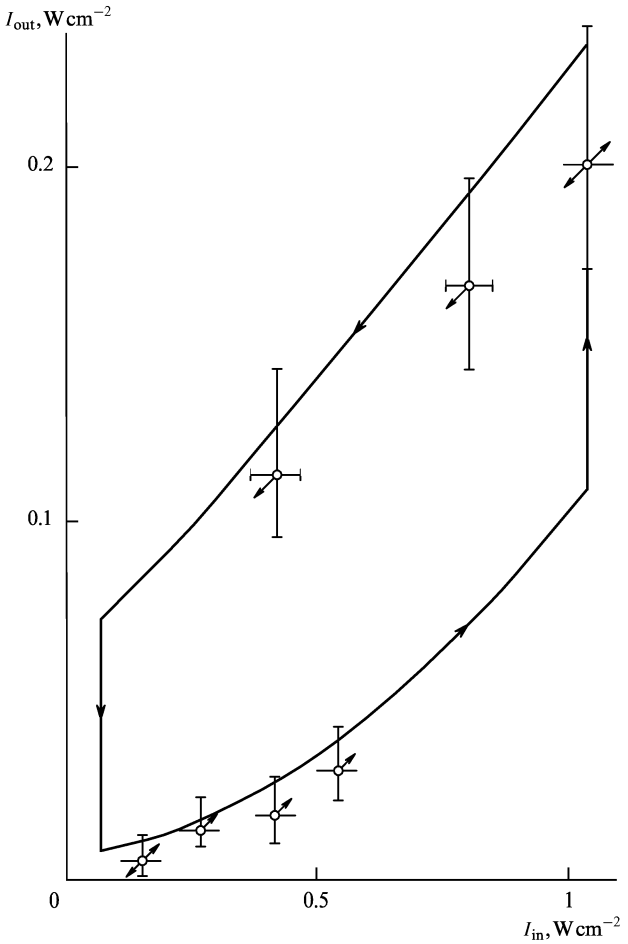

Figure 21. Dependence of intensity I_{out} of ultrasound at the resonator exit. The arrows identify the direction of change of the input intensity I_{in}; $T_0 = 10\,^{\circ}\mathrm{C}$, $l = 1.2$ cm ($b_1 = 0.9$, $b_2 = 6I_{in}$, $b_4 = 0$, $b_5 = 0.75$). The continuous curve is theoretical and the experimental points are plotted with an indication of the errors.

and the self-induced transparency in an intracavity system. The theoretical model discussed in Section 2.4 takes account of the temperature dependence of the velocity of sound (see Fig. 1), represented by $c(T) = c_0 - (\partial c/\partial T)$, in the investigated azeotropic solution (13% of water) of glycerine, which shifted the normal frequencies of the resonator, distorted the profiles of the resonator modes, and ensured distributed feedback between the forward and reverse waves. Depending on the intensity of the exciting radiation, it was possible to operate the resonator in qualitatively different ways: bistable, self-oscillatory, and stochastic.

These experiments were carried out in a thermally stabilised cell of 20 cm × 6 cm × 4 cm dimensions (Fig. 20). An ultrasonic field in a plane-parallel resonator (of the Fabry–Perot type) was generated by a ceramic piezoelectric transducer (*5*) operating at a resonance frequency of 2 MHz. One of the reflectors in this resonator was the transducer itself and the other was a metal disk (*6*) with the reflection coefficient 0.9. The apertures of both reflectors were $2a = 1.5$ cm. Several axial resonator modes could be fitted within the limits of the resonance curve of this transducer. The resonance base could be varied from 0.6 to 4 cm. The resonator axis was vertical. The transducer was supplied from a stabilised hf oscillator and a power amplifier. The maximum ultrasonic beam power reached 20 W in glycerine. The pressure in the transmitted wave at the exit from the resonator was measured with a wide-band ($\Delta\omega \approx 20$ MHz) piezoelectric transducer (*7*) connected to a voltmeter (*9*), which served as a linear detector. Its output was recorded by an automatic plotter (*10*). The parameters of the transmitted and received signals were monitored with an oscilloscope (*4*) and a frequency water (*3*). Measurements were made on glycerine initially kept at 10 °C ($\delta \approx 0.2$ cm^{-1}, $c_0 \approx 2 \times 10^5$ cm s^{-1}, $\gamma_p = 10^{-2}$ K^{-1}, $\rho = 1.2$ g cm^{-3}, $c_p \approx 4$ J g^{-1} K^{-1}, $\partial c/\partial T \approx 4 \times 10^2$ cm s^{-1} K^{-1}).

These experiments showed that, following the transient stage ($t \geqslant a^2/\chi$), the nature of the dependences in the output intensity I_{out} of sound transmitted by the resonator was governed entirely by the input intensity I_{in}. Steady-state conditions were observed in the range $I_{in} \leqslant 1$ W cm^{-2} ($l = 1.2$ cm). When the input intensity was $I_{in} \leqslant 0.2$ W cm^{-2}, the output intensity I_{out} depended linearly on I_{in} and acoustic bistability (Fig. 21) was observed in the range $0.2 \leqslant I_{in} \leqslant 1$ W cm^{-2} ($1.2 < b_2 < 6$). When the input intensity was increased to 1.5 W cm^{-2} ($b_2 \approx 9$), the output intensity I_{out} varied in an oscillatory manner with time. A further increase in I_{in} initially induced sinusoidal oscillations (Fig. 22a), which were transformed into a sum of harmonics (Fig. 22b). In the range $I_{in} \approx 1.5-2$ W cm^{-2} ($b_2 \approx 9-12$), the changes in the output intensity with time became irregular (Fig. 22c).

An increase in the resonator length reduced the range of the input intensities I_{in} in which regular oscillations were observed. For $l > 4$ cm, the oscillatory regime was no longer observed because of an abrupt transition to stochasticity.

The changes in the intial temperature T_0 and in the initial detuning of the frequency ω_0 from the natural

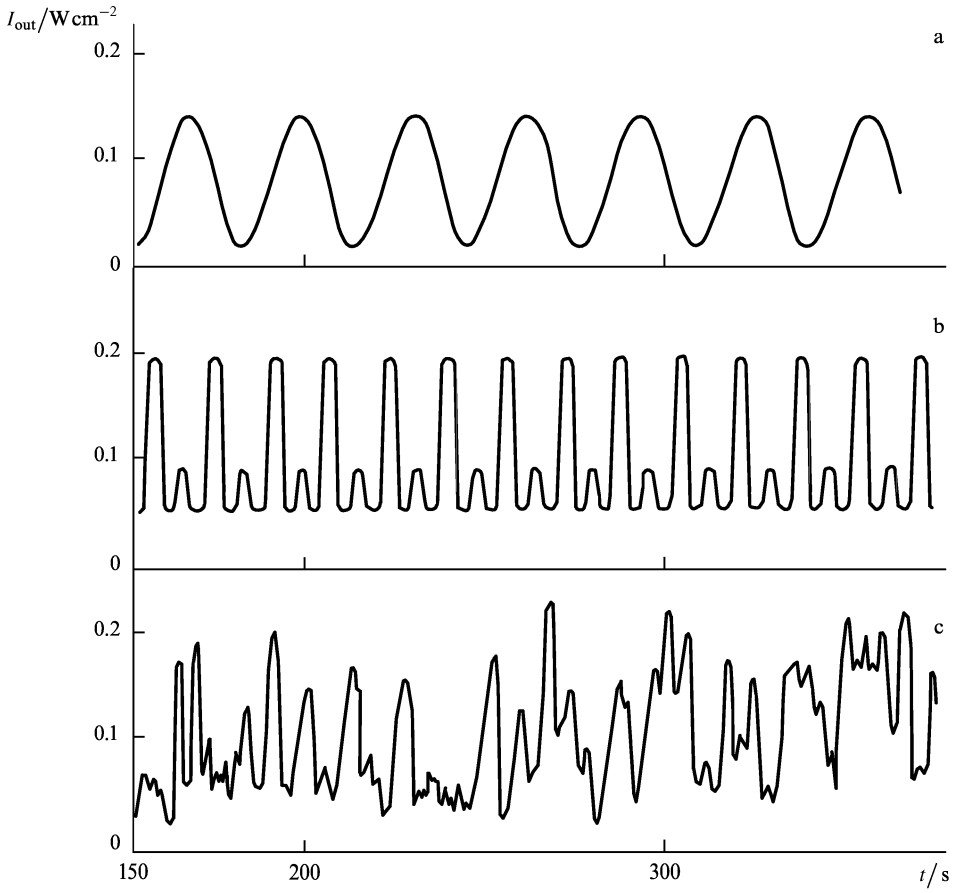

Figure 22. Experimental dependences of the output intensity $I_{out}(t)$: (a) $I_{in} = 1$ W cm^{-2}; (b) $I_{in} = 1.2$ W cm^{-2}; (c) $I_{in} = 2$ W cm^{-2}.

frequency of the resonator did not affect significantly the nature of the time dependence of I_{out}: they influenced only the shape of the hysteresis curve and the spectrum of self-oscillations.

The thermal nonlinearity mechanism played a decisive role in the resonator configuration for the self-excitation of ultrasound in a viscous liquid. At input intensities I_{in} in the range $5-15$ W cm^{-2} a process of self-tuning of the resonator to the pump frequency was observed. This increased, with time, the intensity of the wave transmitted by the resonator to a value corresponding to the transmission maximum. Such self-tuning was observed at pump frequencies very different not only from the frequency corresponding to the transmission maximum of the unexcited resonator, but also from the resonance frequency of the unloaded ceramic piezoelectric transducer. Self-tuning was observed [27] at pump frequencies from 0.8 to 2.1 MHz when the resonance curve of the transducer was 40 kHz. It should be pointed out that acoustic flow induced by the propagation of powerful sound in an absorbing medium did not prevent self-tuning of the resonator.

Effective sound-induced self-tuning of a resonator, filled with a viscous liquid and coupled to a transducer, makes it possible to generate a strong ultrasonic field at a frequency other than the resonance frequency of the transducer, but equal to one of the nature frequencies of the transducer–resonator system. Moreover, this frequency may be altered in a specific manner by self-tuning of the resonator. This approach is promising for the construction of wide-band sources of powerful ultrasound with continuous tuning of the central frequency.

3.5 Nonlinear thermal refraction under shock-formation conditions

The first series of experiments [13, 17, 18, 28, 29] was followed by the work of other experimental groups [34, 35] confirming the main results of the theory [9]. This theory is the only one that makes it possible to analyse the results of investigations of the self-action of ultrasound in liquids. These results showed that the parameters of a source of ultrasound and of a medium, which can be one of the fairly common liquids, may be selected so as to cross the self-focusing threshold without activating other competing sound-induced effects.

It is shown in Sections 2.1 and 3.2 that, in fact, only the use of an optical system for measuring the parameters of an ultrasonic beam makes it possible to reveal, after a reasonable number of measurements, the compression of a wave packet which occurs simultaneously in space and time. However, even in this case the competing nonlinear processes limit the ultimate self-compression capabilities.

Investigations of such processes represent a separate field of problems which have been studied sufficiently in their pure form. Experiments on cascade generation of harmonics under thermal self-action conditions [36, 37] are an example of a comprehensive approach. A detailed description of the results obtained is outside the scope of the present paper; a plan to review these results is mentioned in Ref. [38].

4. Applications

The results presented in Section 3.4, which summarise a series of physical investigations of the thermal self-action of sound in liquids, suggest also quite explicitly the applications of such nonlinear phenomena. All the applications presuppose to a greater or lesser extent the use of the main consequence of the effects described in Sections 2 and 3, which is the possibility of achieving — for a short time — controlled concentration of acoustic energy at a given depth and in a small volume. Moreover, the frequency of sound can be controlled if a resonator is used.

4.1 Precision acoustic methods and ultrasonic devices

We must begin by mentioning first the high efficiency (in acoustic experiments) of laser methods, particularly transient ones, for the visualisation of ultrasonic beams. The progress made in studies of the self-action of sound has been largely due to these particular methods, which provide solutions to the problems of monitoring and control of the effects of sound on a medium in real time and with high precision. It is therefore clear that laser visualisation methods should be included in practically all stages of the development of applications.

The investigated nonlinear effects provide, in turn, the basis for a series of high-precision and fast methods of acoustic measurements. The reliably established and clearly interpreted relationship between the self-concentration parameters (Sections 2.3 and 3.3) and the parameters of both the input sound and of the medium make it possible to apply a new method for the determination of the absolute value of the amplitude of the acoustic pressure at acoustic intensities from 10^{-2} to $20-30$ W cm^{-2} throughout the whole meghertz range [39]. The existing methods can ensure that the error does not exceed 10%, so that the search for new possibilities is very topical. A natural setup would involve the propagation of an acoustic wave through a standard liquid in which the absorption would fall with increase in temperature and, therefore, it would control the intensity of the wave itself. The relative change in time in the pressure amplitude by a factor of K at a given distance L, measured in the direction of propagation from the source, is an informative parameter. The error of the method is estimated to be $1\%-5\%$, depending on the precision with which the parameters of the standard medium are determined.

A bistable resonator, coupled acoustically to a transmitting transducer and filled with a viscous liquid characterised by a strong temperature dependence of the absorption of sound (described in Sections 2.4 and 3.4), may prove useful in acoustic tomography systems where the main component is a precision ultrasonic transducer. A further improvement in the quality of such a resonator transducer, extending the capabilities of tomography, may result from the self-concentration effect, which can increase the focal spot contrast by one or two orders of magnitude on the basis of the data given in Sections 2.2 and 3.3).

4.2 Biotechnology

The strongly local nature of the controlled acoustic interaction with a viscous medium, ensured by the self-action of ultrasound, has attracted the attention of those developing acoustic methods for biotechnology. One of the examples is sound-induced formation of membranes from lipids in a buffer solution [40]. The process occurs as a result of ultrasonic insonation of a mixture and its

effectiveness depends on the type of the lipid, on the ultrasound power (typical values are $P = 30-50$ W), and on the duration of insonation (10 s–5 min per 1–5 ml of the solution). For a given power, the average molecular mass of membranes (i.e. their average size) is governed by the time (energy) of insonation [41]. The use of the self-action effects in a suitable buffer solution makes it possible to control the rate of formation of membranes, the spatial distribution and the mass.

This control of membrane formation, which is the basis of a wide range of biotechnologies, should help in identification of the mechanisms of sound-induced formation of membranes and micelles which are not yet understood. A decisive factor seems to be the mutual attraction of the lipid molecules in the field of local acoustic flow (transient Bernoulli mechanism). A detailed investigation, which should be carried out, can be made only by the methods of local acoustic interaction.

A typical biomolecular medium is indeed a high-viscosity liquid solution. Its main component is in the form of large molecules (which may be proteins) that tend to form ordered structures in a certain temperature range. Therefore, their acoustic spectrum contains characteristic relaxation-type bands. Such liquid-crystal structures are objects suitable for trying out the acoustic self-concentration effects. In fact, estimates show [42] that the temperature derivatives of the velocity of sound, and, particularly, of the absorption in typical liquid crystals in the pretransition transparent phase, are quite high, and the threshold conditions for the observation of the self-action of ultrasound can be satisfied. Therefore, nonlinear ultra-acoustics of biomolecular media represents a wide field for promising research by the methods described in Section 3.

4.3 Medicine

In medicine it is necessary to approach acoustic applications with extreme caution: each application requires a detailed investigation subject to specific limits.

The history of acoustic treatment methods in medicine extends over many decades, but only after 1920, when P Langevin showed [43] that piezoelectric media can be used for the generation of ultrasound, did extensive applications of ultrasound begin to appear in medical diagnostics, therapy, and specific studies of the bioeffects induced by intense ultrasonic waves [44]. The range of applications of acoustic methods in biomedicine and clinical practice has since widened considerably. Ultrasound is being used successfully in the diagnostics and fragmentation of stones in hollow organs, in three-dimensional acoustic tomography, in hyperthermal treatment of cancerous tumors, in speeding up healing of broken bones, and in many other branches of traditional medicine (see, for example, Ref. [45]). Ultrasonic methods and instruments, based on fundamental progress made in physical acoustics, make it possible to diagnose the behaviour of biological objects and are used increasingly in clinical practice. This, in turn, makes it necessary to widen investigations of the mechanisms and qualitative features of the action of ultrasound on the structure and properties of tissues. Biological tissues are complex heterogeneous media which are strongly nonlinear and the nonlinearity applies in particular to thermal and acoustic properties [46]. It would be desirable to employ nonlinear processes that appear during propagation of ultrasonic waves in liquid media, because they may lead to new methods which take account of the nonlinear behaviour of biological tissues.

High-intensity ultrasound damages biological tissues by cavitation or thermal effects, depending on the intensity and duration of action of acoustic waves. The traditional methods for the concentration of ultrasound, even in the best focusing devices used in medical applications [47], are insufficient to establish a regime of an acoustic scalpel because the dimensions of the focusing region (at least several millimetres) are too large and because the structure of this region is not smooth (it is affected by diffraction). Therefore, the action of powerful ultrasound on biological tissues is limited to the action of pulses on solid nodules. This can be done by employing a focused but nonmonochromatic wave with its spectrum in the range hundreds of kilohertz to several megahertz. Such action has a very undesirable influence on the surrounding biological structures which are insonated by the side lobes of the angular distribution of an ultrasonic beam. Ultrasound is used in surgery to ease the motion of a scalpel by vibrating it at a frequency of about 100 kilohertz. Ultrasound may be used in resection of tissues in surgical operations if strong focusing of an ultrasonic wave, without a diffraction structure of the focal spot, and a sufficient intensity of the interaction is ensured.

The self-concentration of powerful ultrasonic radiation makes it possible to focus an acoustic beam in a region of transverse dimensions of the order of 0.1 mm without a diffraction structure of the focal spot (Section 3.3). Hence, it should be possible to construct a device capable of ensuring the action of high-intensity sound on deep layers in biological tissues without damage to the surface layers. Ultrasonic resection by this method would avoid thermal burns and mechanical injury to the surrounding tissues, and yet ensure controlled local coagulation of blood. The difference between the acoustic properties of tissues should make it possible to act selectively on different types of tissues. One could vary the geometric dimensions and localisation of a zone of high intensity of the ultrasonic field, and to control the depth, length, and shape of a section and the rate of cutting.

One other possible field of application is ultrasonic reflection therapy in one of the very few more or less successful branches of nontraditional medicine. Its methods reduce to thermal action on surface tissues or mechanical action on surface or deeper layers of biotissues in what are called biologically active zones. These zones have a distributed structure: the diameter of such a zone is 0.2–2 mm and its depth may exceed 1–2 cm. It is therefore obvious that methods have to be developed for concentrating the action within the whole volume of a biologically active zone. These methods should provide means for altering the geometric parameters of the interaction region, and for the control of the intensity and duration of such action. The solution may include, in our opinion, nonlinear methods for the control of ultrasound described above if supplemented by detailed biomedical investigations. The self-concentration of ultrasound of frequency of the order of 10 MHz satisfies fully the localisation requirements.

5. Conclusions

The acoustic phenomena described above appear most clearly in quasistructural liquids whose physical properties depend strongly on the kinetics of the intermolecular bonds. It is therefore natural to concentrate on nonlinear acoustic phenomena, so that the properties of systems of these bonds in various liquid media are determined. In view of this, aqueous solutions of molecules which form hydrogen bonds with the H_2O molecules deserve the closest attention from the physical and the biophysical (discussed above) points of view. On the one hand, such solutions have striking nontrivial properties: they split into layers, because of the formation of long-lived associates, on increase in temperature (see, for example, Ref. [48]) and not the other way round, as is typical of liquids. The considerable role of the entropy effects in the formation of bonds is responsible for their active participation in biological processes. Theoretical dynamics of such liquid media is essentially limited so far to phenomenological treatments, and approaches to the development of models of separation into layers with increase in temperature have simply been suggested [49]. On the other hand, it is the presence of bonds that (as pointed out above) is responsible for the strong temperature dependence of the acoustic parameters. This in turn appears in the acoustic self-action effects. Therefore, determination of the parameters of these effects is an essential and in our opinion promising part of the investigation of the physics of associated liquids.

Acknowledgements. We are grateful to O V Umnova for valuable discussions.

This review was prepared with partial support from the Russian Fund for Fundamental Research (Grant No. 93-02-15458).

References

1. Landau L D, Lifshitz E M, Pitaevskii L P *Electrodynamics of Continuous Media* 2nd edition (Oxford: Pergamon Press, 1984)
2. Askar'yan G A *Zh. Eksp. Teor. Fiz.* **42** 1567 (1962) [*Sov. Phys. JETP* **15** 1088 (1962)]
3. Akhmanov S A, Sukhorukov A P, Khokhlov R V *Usp. Fiz. Nauk* **93** 19 (1967) [*Sov. Phys. Usp.* **10** 609 (1968)]
4. Lugovoi V N, Prokhorov A M *Usp. Fiz. Nauk* **111** 203 (1973) [*Sov. Phys. Usp.* **16** 658 (1974)]
5. Askar'yan G A *Usp. Fiz. Nauk* **111** 249 (1973) [*Sov. Phys. Usp.* **16** 680 (1974)]
6. Raizer Yu P (Ed.) *Effects of Laser Radiation* (Collection of translations into Russian) (Moscow: Mir, 1968)
7. Pilipetskii N F, Rustamov A R *Pis'ma Zh. Eksp. Teor. Fiz.* **2** 88 (1965) [*JETP Lett.* **2** 55 (1965)]
8. Askar'yan G A *Pis'ma Zh. Eksp. Teor. Fiz.* **4** 144 (1966) [*JETP Lett.* **4** 99 (1966)]
9. Bunkin F V, Lyakhov G A *Tr. Fiz. Inst. Akad. Nauk SSSR* **156** 3 (1984)
10. Zarembo L K, Krasil'nikov V A *Vvedenie v Nelineinuyu Akustiku* (Introduction to Nonlinear Acoustics) (Moscow: Nauka, 1966)
11. Bakhvalov N S, Zhileikin Ya M, Zabolotskaya E A *Nelineinaya Teoriya Zvukovykh Puchkov* (Nonlinear Theory of Acoustic Beams) (Moscow: Nauka, 1982)
12. Bunkin F V, Kravtsov Yu A, Lyakhov G A *Usp. Fiz. Nauk* **149** 391 (1986) [*Sov. Phys. Usp.* **29** 607 (1986)]
13. Assman V A, Bunkin F V, Vernik A V, et al. *Pis'ma Zh. Eksp. Teor. Fiz.* **41** 148 (1985) [*JETP Lett.* **41** 182 (1985)]
14. Bunkin F V, Lyakhov G A, Shuman O B *Pis'ma Zh. Tekh. Fiz.* **8** 1048 (1982)] [*Sov. Tech. Phys. Lett.* **8** 451 (1982)]
15. Bunkin F V, Vlasov D V, Lyakhov G A, et al. *Phys. Lett. A* **101** 95 (1984)
16. Bunkin F V, Lipkin A I, Lyakhov G A *Pis'ma Zh. Tekh. Fiz.* **9** 714 (1983) [*Sov. Tech. Phys. Lett.* **9** 307 (1983)]
17. Assman V A, Bunkin F V, Vernik A V, et al. *Akust. Zh.* **32** 138 (1986) [*Sov. Phys. Acoust.* **32** 86 (1986)]
18. Assman V A, Bunkin F V, Lyakhov G A, et al. *Akust. Zh.* **35** 543 (1989) [*Sov. Phys. Acoust.* **35** 316 (1989)]
19. Assman V A, Bunkin F V, Lyakhov G A, Proskuryakov A K, Shipilov, K F, Umnova O V *Opt. Acoust. Rev.* **1** 205 (1990–1991)
20. Zabolotskaya E A, Khokhlov R V *Akust. Zh.* **22** 28 (1976) [*Sov. Phys. Acoust.* **22** 15 (1976)
21. Bunkin F V, Volyak K I, Lyakhov G A *Zh. Eksp. Teor. Fiz.* **83** 575 (1982) [*Sov. Phys. JETP* **56** 316 (1982)]
22. Kikoin I K (Ed.) *Tablitsy Fizicheskikh Velichin: Spravochnik* (Tables of Physical Quantities: Handbook) (Moscow: Atomizdat, 1976)
23. Krivokhizha S V, Fabelinskii I L *Zh. Eksp. Teor. Fiz.* **50** 3 (1966) [*Sov. Phys. JETP* **23** 1 (1966)]
24. Lyakhov G A, Shipilov K F, Umnova O V *J. Phys. IV Colloq.* **4** 1201 (1994)
25. Lyakhov G A, Shipilov K F, Umnova O V *J. Phys. IV Colloq.* **4** 1197 (1994)
26. Firth W J, Wright E M *Opt. Commun.* **40** 233 (1982)
27. Lykhov G A, Proskuryakov A K, Umnova O V, et al. *Akust. Zh.* **39** 299 (1993) [*Acoust Phys.* **39** 158 (1993)]
28. Assman V A, Proskuryakov A K, Shipilov K F *Akust Zh.* **36** 586 (1990) [*Sov. Phys. Acoust.* **36** 331 (1990)]
29. Assman V A, Bunkin F V, Vernik A V, et al. *Akust Zh.* **32** 754 (1986) [*Sov. Phys. Acoust.* **32** 472 (1986)]
30. Riley W A Jr, Love L A, Griffith D W *J. Acoust. Soc. Am.* **71** 1149 (1982)
31. Lyakhov G A, Proskuryakov A V, Umnova O V *Akust. Zh.* **36** 502 [1990] [*Sov. Phys. Acoust.* **36** 279 (1990)]
32. Belen'kaya O V Zhileikin Ya M, Lyakhov G A, et al. *Akust. Zh.* **38** 984 (1992) [*Sov. Phys. Acoust.* **38** 539 (1992)
33. Gibbs H M *Opticaal Bistability: Controlling Light with Light* (New York: Academic Press, 1985)
34. Bukhshtaber V M, Pivovarov V A, Stefanov S R *Akust. Zh.* **33** 376 (1986) [*Sov. Phys. Acoust.* **32** 231 (1986)]
35. Andreev V G, Karabutov A A, Rudenko O V, Sapozhnikov O A *Pis'ma Zh. Eksp. Teor. Fiz.* **41** 381 (1985) [*JETP Lett.* **41** 466 (1985)]
36. Karabutov A A, Rudenko O V, Sapozhnikov O A *Akust. Zh.* **35** 67 (1989) [*Sov. Phys. Acoust.* **35** 40 (1989)]
37. Rudenko O V, Sagatov M M, Sapozhnikov O A *Zh. Eksp. Teor. Fiz.* **98** 808 (1990) [*Sov. Phys. JETP* **71** 449 (1990)]
38. Rudenko O V, in *Proceedings of Thirteenth International Symposium on Nonlinear Acoustics, Bergen, 1993* (Ed. H Hobak) (Singapore, World Scientific, 1993)
39. Assman V A, Bunkin F V, Lyakhov G A, Proskuryakov A K, Shipilov K F "Method for determination of the absolute amplitude of the pressure on an acoustic wave", USSR Author's Certificate No. 1 772 631 (1992), Appl. 12.12.1990, Publ. 30.10.1992
40. Onisi S, in *Seitai Kobanski (Biopolymers)* Ed. Y Imanishi (Tokyo, Kyoritsu Shuppan, 1985) p. 353 of translation into Russian (Moscow: Mir, 1988) p. 353
41. Herrman U, Fendler J *Chem. Phys. Lett.* **64** 270 (1979)
42. Lyakhov G A, Umnova O V *Akust. Zh.* **40** 314 (1994) [*Acoust. Phys.* **40** 286 (1994)]
43. Langevin P, British Patent N.S., 457 No. 145691 (1920)
44. Muir T G, Carstensen E L *Ultrasound Med. Biol.* **6** 345 (1980)
45. Landini L, Varrazzani L *IEEE Trans. Ultrason. Ferroelectr. Freq. Control* **37** 448 (1990)
46. Kazakov V V, Klochkov B N *XI Mezhd. Simp. po Nelineinoi Akust.*, Novosibirsk, 1987 (Eleventh International Symposium on Nonlinear Acoustics, Novosibirsk, 1987) Vol. 2, p. 29
47. ter Haar G, Sinnett D, Rivens I *Rev. Med. Biol.* **34** 1743 (1989)
48. Vedenov A A *Fizika Rastvorov* (Physics of Solutions) (Moscow: Nauka, 1984)
49. Lyakhov G A *Pis'ma Zh. Eksp. Teor. Fiz.* **60** 93 (1994) [*JETP Lett.* **60** 99 (1994)]